Unequal scaling of urban vegetation cooling across sociodemographic groups

Yuyang Chang [1*], Gabriele Manoli [2], Alby D. Rocha [3], Jonas Schwaab [4], Maarten J. van Strien[5], Dominic A. Martin [6], Ronita Bardhan [7], Jaboury Ghazoul [1], Fritz Kleinschroth [4*]

1 Ecosystem Management, Department of Environmental Systems Sciences, ETH Zurich, Zurich, Switzerland

2 Laboratory of Urban and Environmental Systems, École Polytechnique Fédérale de Lausanne, Lausanne, Switzerland

3 Earth Observation and Geoinformatics Division, INPE - National Institute for Space Research, São José dos Campos - SP, Brazil

4 Institute for Environmental Planning, Leibniz Universität Hannover, Hannover, Germany

5 Planning of Landscape and Urban Systems, Department of Civil, Environmental and Geomatic Engineering, ETH Zurich, Zurich, Switzerland

6 Department of Environmental Sciences, Wageningen University, Wageningen, Netherlands

7 Sustainable Design Group, Department of Architecture, University of Cambridge, Cambridge, United Kingdom

Corresponding author*

Yuyang Chang, email: yuyangchang.yc@gmail.com

Fritz Kleinschroth, email: kleinschroth@umwelt.uni-hannover.de

This paper is a **non-peer-reviewed** preprint submitted to EarthArXiv.

Abstract

Urban vegetation mitigates heat in cities, but its benefits often reach disadvantaged residents least, an inequality of growing concern as climate change intensifies urban heat. Whether residence-based cooling exposure and its inequality scale systematically with population size and density, as infrastructural and socioeconomic attributes do, remains unclear. Here, we simulate process-based vegetation cooling and quantify residential exposure across radii using seven million geocoded census records covering urban Switzerland. Mean cooling per resident decreases in denser and more populous areas, with steeper declines among socioeconomically disadvantaged residents and temporary-permit holders. Cooling inequality rises with population size and density. An equity typology combining inequality magnitude and social direction identifies priority municipalities and 1-km² cells, with over a third of municipalities classified as high-inequality and pro-advantaged for both socioeconomic position and residence status. Our findings reveal that both vegetation-cooling inequality and the social stratification of cooling are emergent scaling properties of cities.

Main

Urban vegetation is a frontline tool for climate adaptation, providing canopy shade and evapotranspirative cooling that reduce heat exposure and improve well-being in urban areas[1,2]. However, low-income and minority communities generally face higher ambient temperatures and have fewer resources to adapt[3,4]. Urban vegetation access is itself heterogeneously stratified[5]: socially disadvantaged residents tend to live in areas with less green cover, with fewer heat adaptation options[6,7]. As urban heat risks are projected to intensify under climate change[8], ensuring equitable distribution of vegetation cooling benefits has become a key challenge for climate-resilient cities.

Even within the same urban area, residents may receive markedly different vegetation-cooling benefits around their homes, and these differences may align systematically with socioeconomic and demographic characteristics. Assessing such distributive equity requires fine-resolution climate, vegetation data, and geocoded demographic information, three data streams that are rarely combined at national scale in a single analysis. Most assessments of urban vegetation cooling rely on satellite-based proxies such as NDVI or land surface temperature[9,10], which capture broad spatial patterns but are indirect measures of actual microclimatic conditions[11]. Field-based sensor campaigns provide more direct observations[12,13], but remain spatially sparse and are rarely linked to demographic information. Process-based models, such as ENVI-met[14], simulate canopy shading and evapotranspiration more accurately, but their high computational demands at the neighborhood scale have limited their use for national-scale assessment of distributive justice in vegetation-cooling benefits. On the demographic side, socioeconomic data are generally available only at coarse administrative units[15,16]. Unpopulated zones within large administrative boundaries inflate the apparent cooling available to residents, and aggregation effects can obscure within-neighborhood contrasts and misrepresent individual exposure[17]. Furthermore, administrative-unit-level data cannot accurately capture residents' immediate cooling environments across different radii around their homes[18]. Geo-coded individual-level microdata would enable direct linkage of residential location to cooling environment, but privacy constraints make such data rarely available at population scale[19].

Yet precise individual-level measurements alone cannot reveal whether cooling patterns generalize across cities of different sizes. Guiding equitable cooling interventions requires understanding how per-resident vegetation cooling is distributed along the population gradient and whether this varies across social groups. Urban scaling laws provide a generalized framework for such complex distributional challenges[20]. Originally developed to describe how city-level properties vary systematically with total city population, scaling analysis has revealed that cities follow consistent regularities regardless of their cultural and geographic context[21]. Socioeconomic quantities such as GDP, innovation and crime often scale superlinearly, meaning that their per capita levels tend to increase with city size[22,23], whereas many infrastructural quantities scale sublinearly, consistent with economies of scale in infrastructure provision[24]. These regularities have since been extended to urban environmental outcomes, including waste generation[25] and air pollution[26]. Urban scaling laws have also been applied to test the within-city and across-city urban inequality distributions of human networking, productivity, and infrastructure[27,28]. Most recently, scaling has been applied to urban climate, showing that intra-urban temperature variability follows general scaling functions across cities worldwide[29]. Recent global evidence also shows that intra-urban inequalities in land surface temperature and green-space area scale with population[30]. However, how vegetation cooling scales with population and how this scaling varies across social groups remain largely unexplored.

Europe has experienced increasingly frequent and severe heat events in recent decades, with heat-related mortality rising across the continent[31,32]. Within this warming context, Switzerland, warming at approximately 1.6 times the northern hemispheric average rate[33], presents a particularly timely setting for examining cooling equity, offering a richly diverse sociodemographic profile alongside exceptional individual-level data availability. Foreign nationals account for 27.7% of the permanent resident population, 19.8% are aged 65 or older, and 6.0% are aged 80 or older[34], a composition that naturally stratifies heat vulnerability across multiple demographic dimensions[35]. Evidence from other countries suggests that residents with lower heat-adaptation capacity seek nature-based cooling solutions[36]. In Switzerland, where fewer than 10% of households are air-conditioned [37] and urban green space access is highly unequal[38], the distribution of vegetation cooling benefits is particularly consequential.

Here, we use the process-based Soil Canopy Observation of Photosynthesis and Energy fluxes (SCOPE) model[39] to simulate both the radiative and evapotranspirative components of vegetation cooling across Switzerland at 10 m resolution and link these estimates to geo-coded census records for more than seven million residents of urban and peri-urban municipalities, from small towns to the largest Swiss cities, yielding residence-based cooling exposure for each individual. We characterize how cooling exposure varies across five sociodemographic indicators, residence permit type, civil status, age, gender and socioeconomic position, and across spatial extents of 20-1,000 m around each residence. We then test whether mean per-resident cooling declines with population size and density, and whether cooling scaling differs by socioeconomic position and residence permit status. Finally, we apply a joint Gini-Concentration Index framework at both municipal and 1 km² cell levels to identify locations where cooling benefits are both highly unequal and disproportionately concentrated among advantaged groups, providing a dual diagnostic for equitable greening interventions. Cities are known to concentrate advantage as they grow, and this work tests whether the cooling that vegetation supplies is concentrated in the same way, and whether the residents left with the least are the same from one city to the next.

Results

Geography of vegetation cooling across Switzerland

Cooling benefits from urban vegetation exhibited strong spatial heterogeneity across Switzerland (Fig. 1a). Cooling benefits are quantified using the Greening Cooling Services (GCoS) index, a unitless 0-1 metric integrating vegetation's radiative and evapotranspirative cooling at 10 m resolution, derived from an hourly process-based simulation (SCOPE model; see Methods), representing the maximum potential cooling supply under peak summer heat conditions. Population-weighted cooling benefits and background air temperatures vary across biogeographical regions and cantons. At the cantonal level (cantons are the 26 states of the Swiss federation), background temperatures vary widely, while average cooling values show a narrower range because the GCoS is a bounded index (Fig. 1b). Cantons that experience high background temperatures (> 26 °C) while still receiving relatively high cantonal-average cooling benefits include Zurich and Basel-Landschaft; the densely built canton of Basel-Stadt, by contrast, combines comparably high temperatures with markedly lower cooling. Cantons like Valais and Jura display the lowest average cooling benefits.

The population's exposure to these cooling benefits is unevenly distributed relative to background heat (Fig. 1c). The vast majority of Swiss residents are concentrated in areas experiencing high mean summer air temperatures, with population exposure peaking strongly near 27 °C. In contrast, the population is disproportionately exposed to only moderate levels of vegetation-induced cooling (peaking between 0.4 and 0.5), with a negligible fraction of residents experiencing high cooling benefits (> 0.7). This uneven demographic exposure is further reflected across biogeographical regions (Fig. 1d). Population-weighted median cooling benefits are highest in the Central Plateau and Jura regions, where background temperatures are also the most severe.

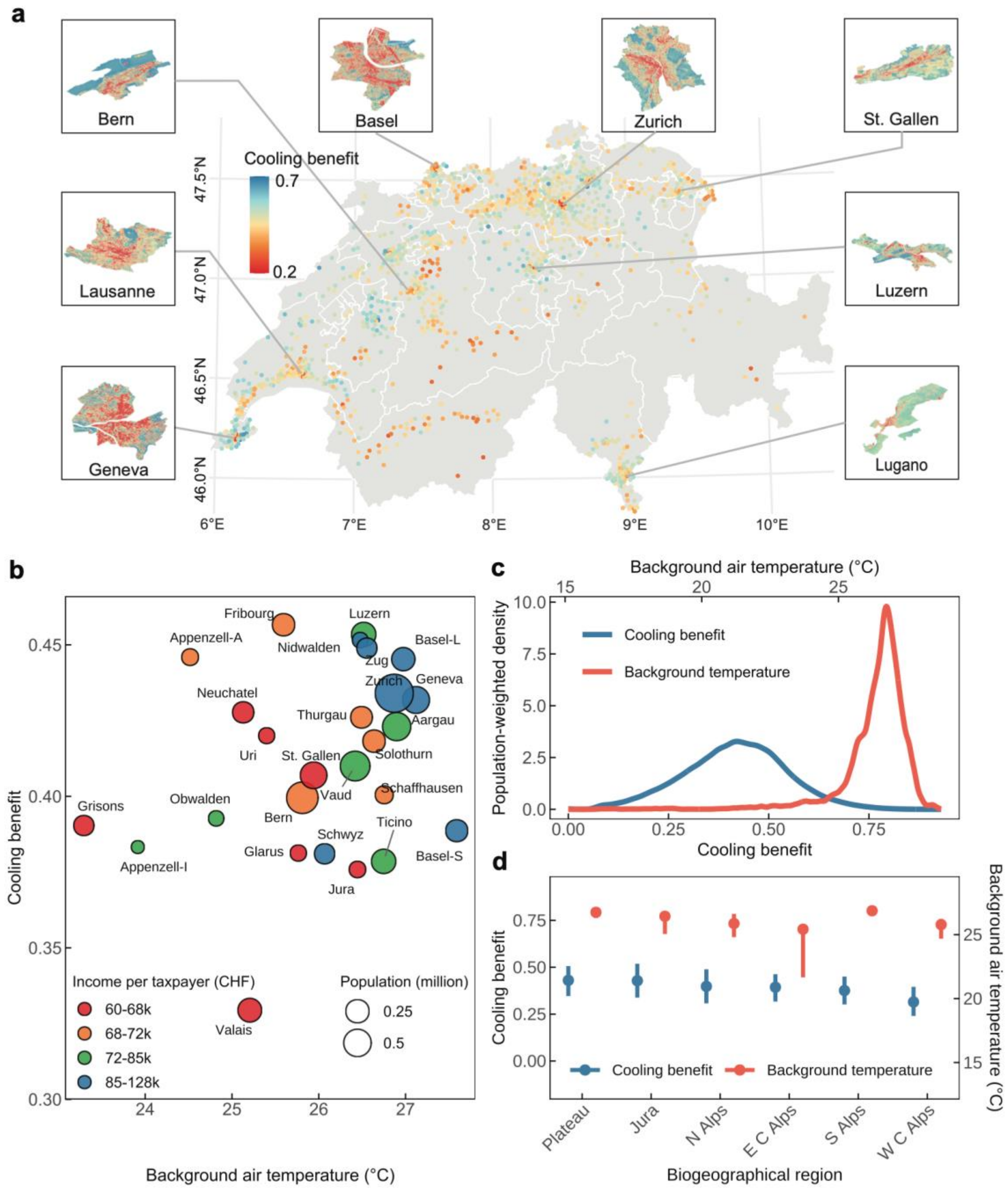

Fig. 1. Geographic and demographic distribution of cooling benefits from urban vegetation across Switzerland. a, Spatial distribution of the cooling benefit (quantified as the unitless Greening Cooling Services index, GCoS) averaged at the municipal level. Insets highlight the spatial cooling patterns within eight major Swiss cities. b, Cantonal-level relationship between population-weighted average cooling benefits, background air temperatures, and income per taxpayer. Bubble size corresponds to the cantonal population (in millions), while color denotes the median income per taxpayer (CHF). c, Population-weighted density

distributions of cooling benefits (blue line, bottom x-axis) and background air temperatures (red line, top x-axis). Background temperature represents the mean air temperature (Ta mean). d, Population-weighted median cooling benefits (blue, left y-axis) and background temperatures (red, right y-axis) across six biogeographical regions of Switzerland. Vertical bars represent the population-weighted interquartile range (25^{th}-75^{th} percentile). Biogeographical regions include the Jura, Central Plateau (Plateau), Northern Alpine Slope (N Alps), Southern Alpine Slope (S Alps), Eastern Central Alps (E C Alps), and Western Central Alps (W C Alps). Municipality and biogeographic region classifications are shown in Extended Data Fig. 1. All analyses are based on 2018, a warm but not extreme summer year that slightly exceeded the upper bound of the ±1 standard deviation range around the 1990-2024 long-term mean Swiss summer temperature (Supplementary Fig. 1).

Cooling benefits from urban vegetation across social groups and distance

We compared residential cooling across five sociodemographic indicators at radii from 20 to 1,000 m. Cooling magnitude differs significantly across all five indicators (Fig. 2a; pairwise statistics in Supplementary Table 1). The widest gaps are found for socioeconomic position and residence permit type, which are of similar magnitude. Cooling is highest among Swiss citizens and high-SEP residents and lowest among short-term (L) permit holders, who have the lowest median of any group examined; the SEP gradient is strictly ordered from high to low. Differences by gender and civil status are detectable but much smaller, and residents aged 26-44 have the lowest cooling exposure among all age groups.

These patterns hold after controlling for all five indicators simultaneously, with SEP and permit type retaining the largest independent cooling deficits in a multiple linear regression (Extended Data Fig. 2). The youngest group was the only exception, with its unadjusted deficit reversing after adjustment. Sociodemographic rank orderings are largely consistent across the full 20-1000 m range (Fig. 2b), with disparities present at the smallest focal radii and persisting across broader extents. The disadvantage of short-term permit holders is the most strongly localized. They start from the lowest median cooling at short radii, rise more steeply than any other permit group, and overtake long-term (B) permit holders at 740 m, so their deficit is concentrated in the immediate residential environment rather than the wider neighborhood. The same asymmetry appears in the distance at which each group approaches its own cooling plateau, which is 141 m for short-term permit holders against 81 m for Swiss citizens, and 99 m for low-SEP against 65 m for high-SEP residents (Extended Data Fig. 3a). Absolute cooling decreases progressively across the low-, medium-, and high-density tertiles for every group, reaching low levels for all groups in the densest tertile. However, SEP and permit-group rankings are preserved within each tertile (Extended Data Fig. 4), suggesting that the two largest disparities are not solely attributable to differences in groups' distributions along the density gradient.

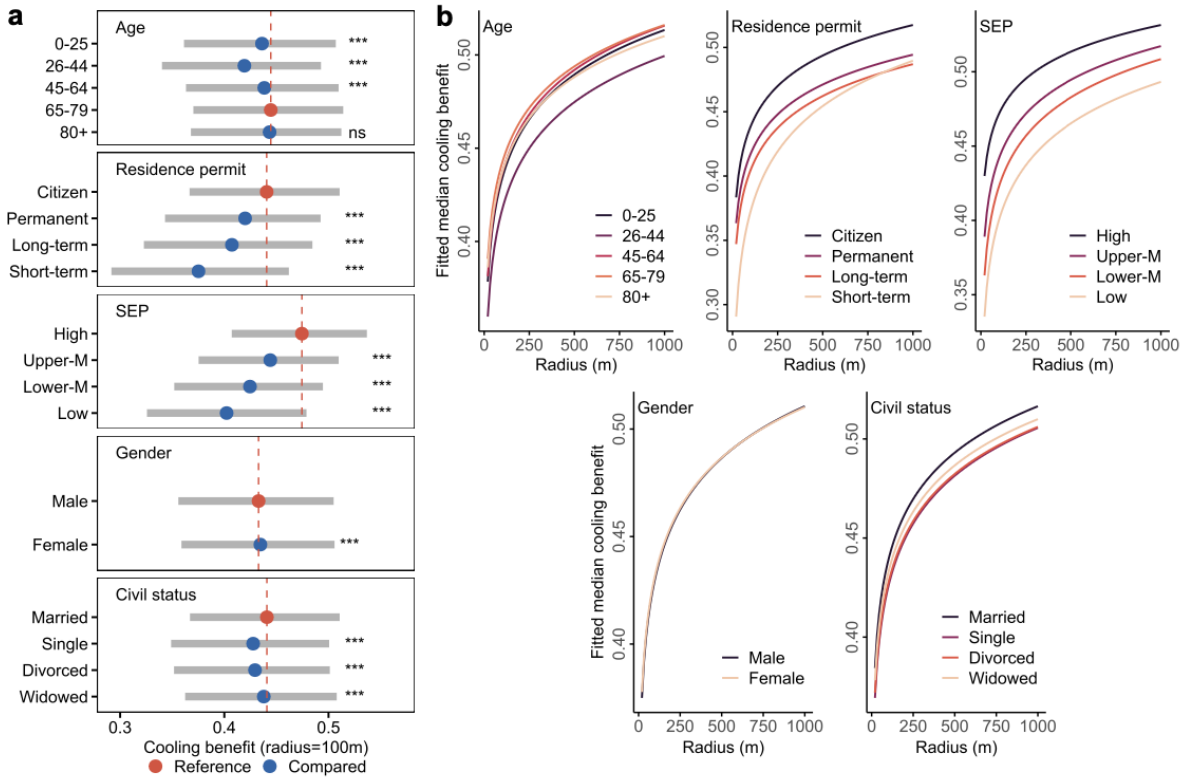

Fig. 2. Sociodemographic disparities in cooling benefits from urban vegetation. a, Median cooling benefit at a focal radius of 100 m, stratified by five sociodemographic indicators: age, residence permit type, socioeconomic position (SEP), gender, and civil status. Points indicate group medians and horizontal bars the interquartile range (25^{th}-75^{th} percentile), shown as a descriptive measure of the spread of the exposure distribution. Red marks the reference group for each indicator and blue the compared groups; the vertical dashed line marks the reference group median. Significance stars refer to pairwise tests against that reference, based on a cluster bootstrap that resamples residential addresses (*** $p < 0.001$, ns not significant); differences and confidence intervals are given in Supplementary Table 1. b, Fitted median cooling benefit as a function of focal radius from 20 to 1,000 m for the same five indicators, from log-linear models of group median cooling on log radius. The

underlying observed medians and interquartile ranges are shown in Extended Data Fig. 3b. Residence permit categories: Citizen = Swiss citizens (passport holders); Permanent = permanent residence permit (C); Long-term = long-term work/study permit (B); Short-term = short-term permit (L).

Socially stratified urban scaling of cooling benefits

A negative scaling exponent ($\beta < 0$) indicates that denser or larger urban areas provide lower per-capita levels of a property. We test whether cooling benefits from urban vegetation scale with population, and whether the scaling exponent differs by social group, at two spatial levels: 1 km^2 cell (population density) and municipalities (population size). Cooling benefits are measured as the mean vegetation cooling at focal radii from 100 to 1,000 m around each residential address.

Mean cooling benefits at a 100 m focal radius decline with population density (β = -0.058; Fig. 3a), indicating that denser areas provide weaker local cooling. Residents with the lowest cooling within each 1 km^2 cell (P10, the 10^{th} percentile of the local cooling distribution; β = -0.078) show a steeper decline with population density than those with the highest (P90; β = -0.044; $\Delta\beta$ = 0.034, $p < 0.001$), indicating that denser environments disproportionately disadvantage those already receiving the least cooling. For residence permit status, permanent residents show a shallower cooling decline than temporary permit holders, though the difference is small ($\Delta\beta$ = 0.003; Fig. 3b). The SEP gradient is more pronounced: High-SEP residents show a shallower decline (β = -0.041) than low-SEP residents (β = -0.067; $\Delta\beta$ = 0.026; Fig. 3c). All group gaps were largest in the immediate residential environment and attenuated at broader extents (Fig. 3a-c insets). When examining the relationship between mean cooling benefits and municipality population size, negative scaling persists but is weaker (β = -0.026; Fig. 3d-f), indicating that population size captures less of the cooling variation than population density. The P10-P90 gap widens ($\Delta\beta$ = 0.048); the permit gap, though small, is more pronounced than at the density level ($\Delta\beta$ = 0.009).

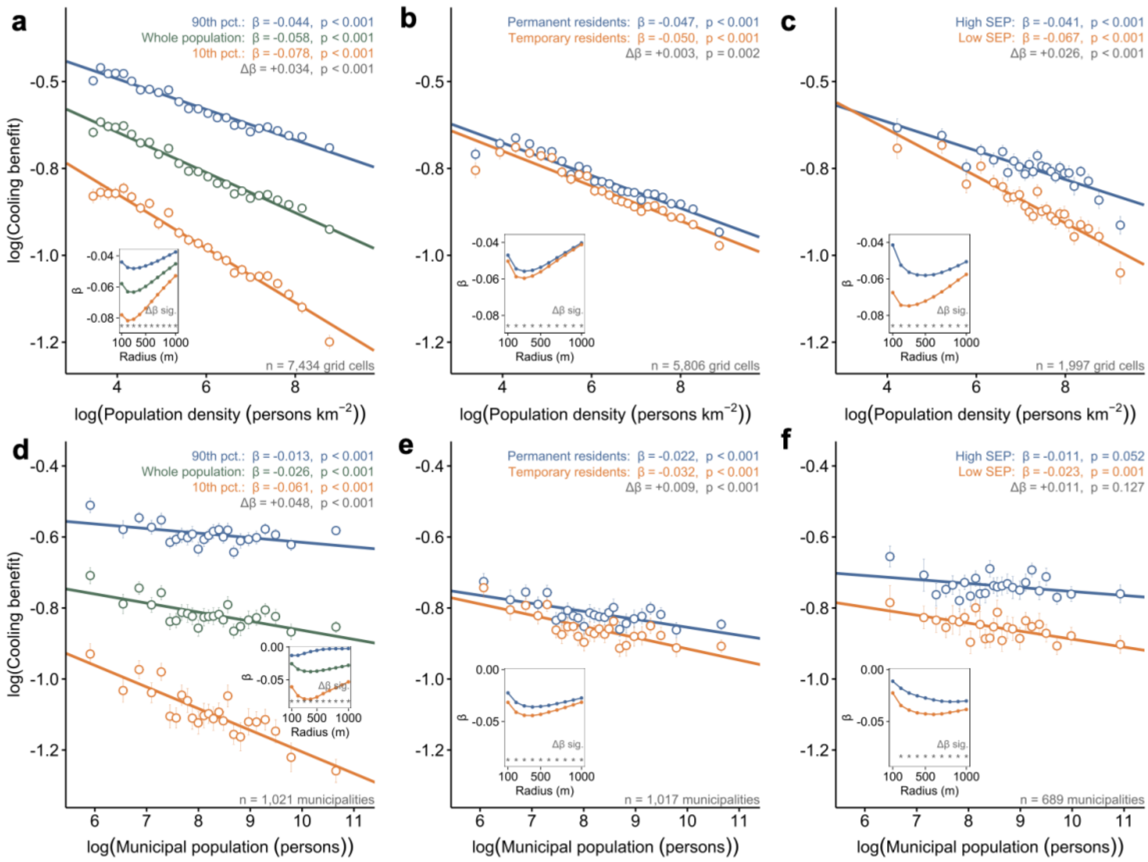

Fig. 3. Socially stratified urban scaling of cooling benefits from urban vegetation. Log-log scaling regressions of mean individual cooling benefits (100 m radius) against population density and size, stratified by social group. Points show means within 25 equal-count bins along the x-axis, with vertical bars giving the standard error of the mean in each bin; binning is for display only, and all regression lines and scaling exponents are fitted to the unbinned data. Panels a-c show results for 1 km² cell level (population density; persons km^{-2}); panels d-f show results for municipalities, where population is the total municipal population. a and d: scaling of the whole population (green), the 90th percentile (90th pct., blue; individuals with the highest cooling exposure within each unit), and the 10th percentile (10th pct., orange; individuals with the lowest cooling exposure). b and e: permanent residents (Swiss citizens and holders of permanent residence permits (C); blue) and temporary residents (orange; permit B and L). c and f: in the top 25% (high SEP, blue) and bottom 25% (low SEP, orange) of socio-economic position (SEP). Insets show scaling exponents estimated across focal radii from 100 to 1,000 m (100 m intervals); significance stars indicate a significant difference in scaling exponents between the two groups (see Methods; *p < 0.05, no * means not significant). R^2 for each log-log model is presented in Supplementary Table 2.

Spatial distribution and scaling of cooling inequality

We examine cooling inequality using the Gini index mapped at both the 1 km^2 cell level and the municipality level (Fig. 4a-b). The Gini index summarizes how unevenly cooling benefits are distributed among the residents of a single unit, on a scale from 0 when every resident receives the same cooling to 1 when it is concentrated on one resident. It is computed within each unit and then related to that unit's population, so it measures inequality inside places. The Gini index scales positively with population size at both levels: at a 100 m focal radius, the scaling exponent is $\beta = 0.126$ at the 1 km^2 cell level and $\beta = 0.081$ at the municipality level (both $p < 0.001$; Fig. 4c), indicating that cooling inequality is greater in more populated units. Results are robust to the choice of inequality measure: an equivalent analysis using the Theil index, an entropy-based alternative to the Gini, yields the same scaling pattern (Extended Data Fig. 5; Supplementary Table 3).

We also compared Gini values between residence permit and SEP subgroups at the 1 km^2 cell level (Fig. 4d-e) and municipality level (Extended Data Fig. 6). For residence permit groups, the Gini index for temporary and permanent residents is closely aligned (slope = 0.95, $R^2 = 0.60$ at 100 m focal radius), indicating similar magnitudes of within-group cooling inequality across residential status groups. For socioeconomic position (SEP), Gini values for residents in the bottom 50% SEP fall systematically below those of the top 50% SEP (slope = 0.43 at a 100 m focal radius; 0.59 at 1,000 m), suggesting that higher-SEP residents exhibit greater heterogeneity in cooling access, while lower-SEP residents are exposed to a narrower range of cooling values. The Theil index confirms the same within-group patterns (Extended Data Fig. 5d-e).

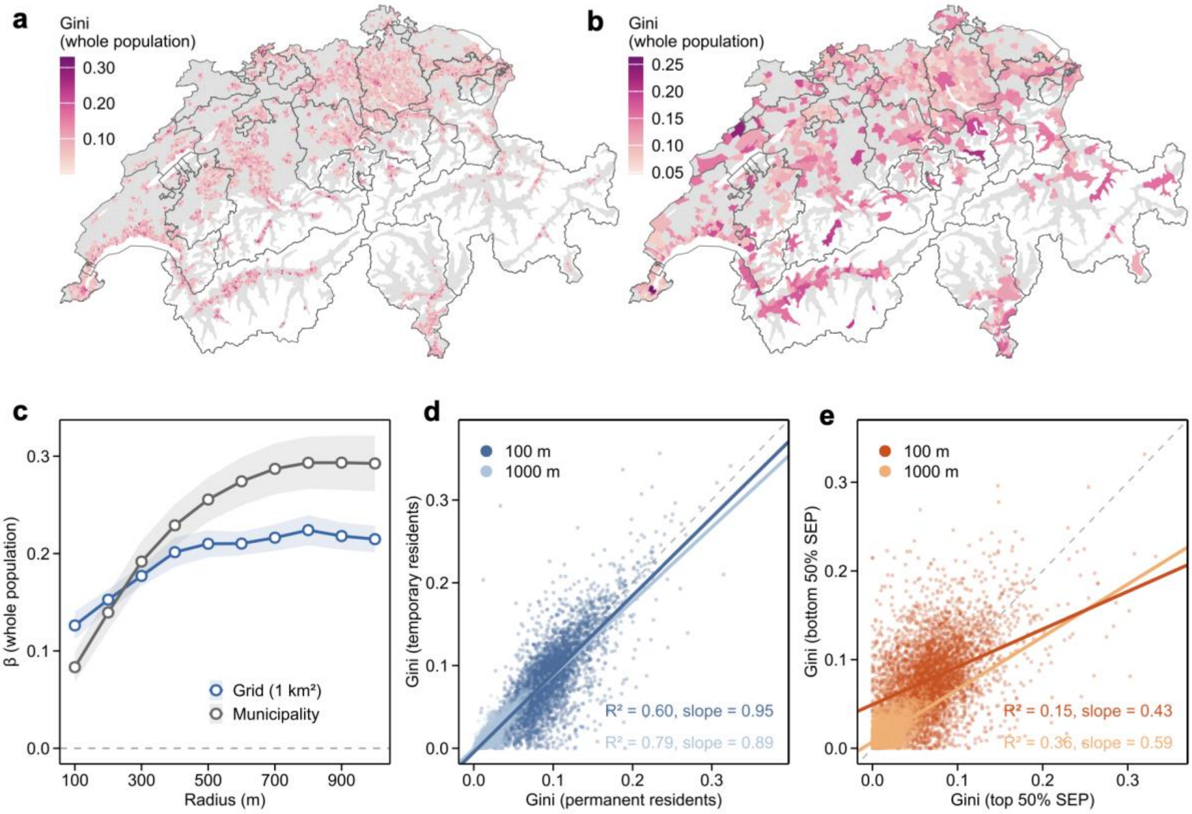

Fig. 4. Spatial distribution and urban scaling of cooling inequality. a-b, Spatial distribution of the Gini index of cooling inequality at (a) the 1 km² cell level and (b) the municipality level, computed at a 100 m focal radius; units with fewer than 20 residents are excluded; cantonal boundaries are shown in dark grey. c, Scaling exponent (β) of the Gini index against population size, estimated at the 1 km² cell (blue circles) and municipality (grey circles) levels across focal radii from 100 to 1,000 m (100 m steps); shaded ribbons show 95% confidence intervals. d-e, Pairwise comparison of subgroup Gini values at the 1 km² cell level, shown at focal radii of 100 m (dark) and 1000 m (light), for (d) temporary versus permanent residents and (e) residents in the bottom 50% versus the top 50% of socioeconomic position (SEP). Dashed lines indicate the 1:1 equality line; solid lines show ordinary least squares regression fits with reported slope and R^2 values.

Cooling equity typology at municipal and 1 km² cell levels

To characterize how cooling inequality and its social distribution co-vary across local contexts, we jointly examine the Gini index and the Concentration Index (CI) in Gini-CI space across all Swiss municipalities (Fig. 5). Higher Gini values indicate greater internal inequality in cooling exposure; the CI captures whether benefits disproportionately favor disadvantaged (negative CI) or advantaged (positive CI) residents. Municipalities show a positive Gini-CI association, indicating that higher cooling inequality typically coincides with cooling favoring socially advantaged populations. This holds for SEP and residence permit status (Fig. 5a, e). The same positive association is observed when focusing on elderly residents, comparing those aged 80+ against the 65-79 group (Extended Data Fig. 7a).

The Gini-CI space yields four cooling equity typology quadrants defined by inequality level and who benefits from cooling. The priority upper-right quadrant, representing above-average inequality combined with pro-advantaged cooling, contains 36% of municipalities for SEP and 39% for permit type (e.g., Geneva and Zurich, respectively; Fig. 5c, g). The largest shares, 42% for SEP and 43% for permit type, fall in the lower-right quadrant, where inequality is below average but cooling still favors advantaged residents. By contrast, 13% and 12%, respectively, occupy the lower-left quadrant, where cooling is more evenly distributed and modestly favors disadvantaged residents (e.g., Horgen and Riehen; Fig. 5d, h). Among elderly residents, 28% of municipalities exhibit above-average inequality with cooling concentrated among residents aged 65-79, whereas 24% exhibit below-average inequality with cooling modestly favoring those aged 80 and above (e.g., Lugano and Frauenfeld, respectively; Extended Data Fig. 7c-d). The corresponding Gini-CI typology for 1-km^2 cells is mapped nationally in Extended Data Fig. 8.

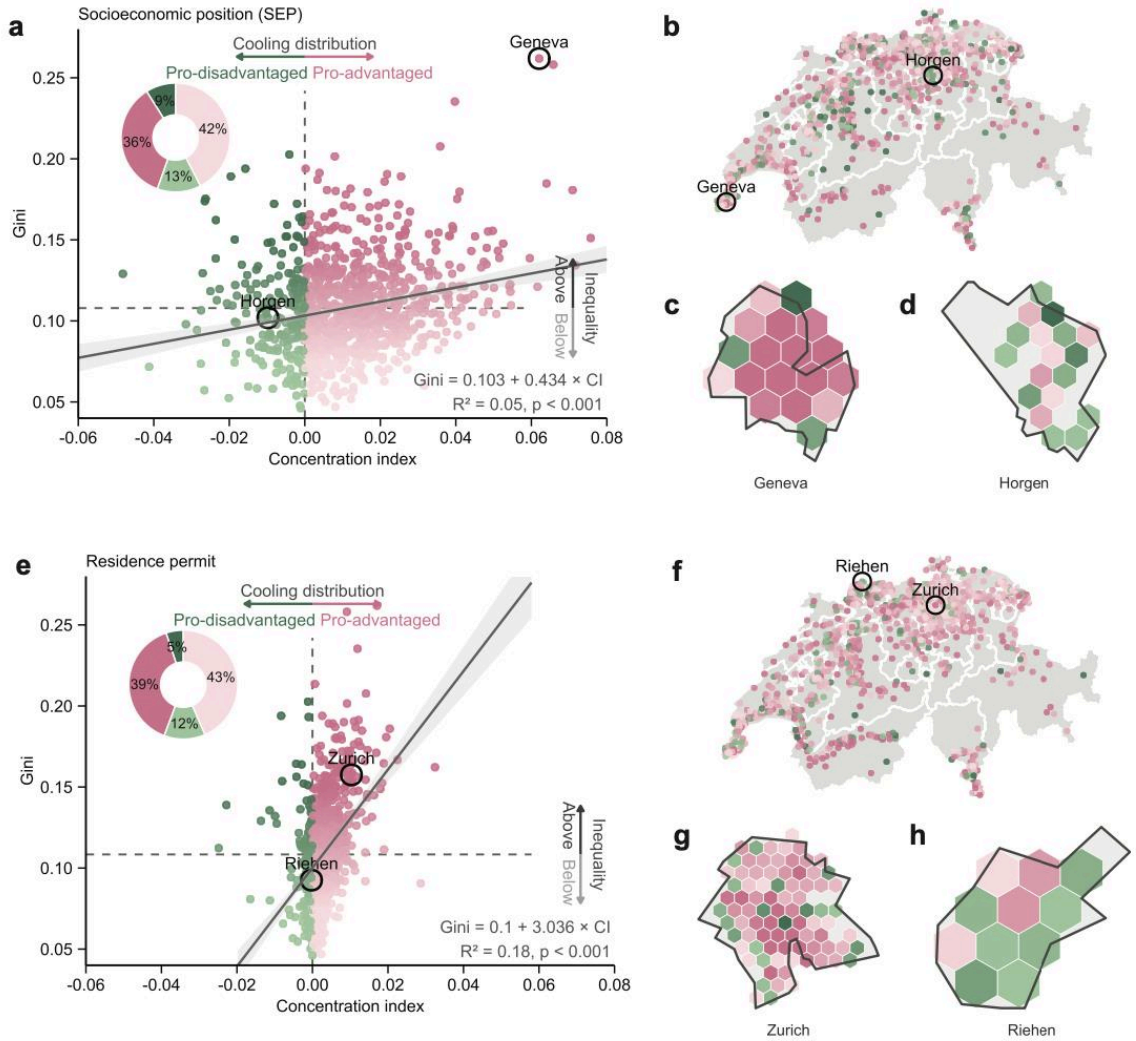

Fig. 5. Municipal-level cooling inequality and equity typology for socioeconomic position (SEP) and residence permit type. a, e, Each point represents one municipality in Gini-CI space; the Gini index (y-axis) measures internal inequality in cooling exposure derived from individual-level 100 m focal cooling, and the Concentration Index (CI; x-axis) captures whether cooling is concentrated among disadvantaged or advantaged residents; positive CI indicates cooling concentrated among advantaged residents. Dashed lines mark the mean Gini (horizontal) and CI = 0 (vertical), dividing municipalities into four quadrants; insets show the percentage of municipalities in each quadrant. Regression lines show fitted linear relationships with 95% confidence intervals. b, f, Geographic distribution of municipalities colored by Gini-CI quadrant; pink indicates the upper-right quadrant (above-average inequality, pro-advantaged) and green indicates the lower-left quadrant (below-average inequality, pro-disadvantaged); selected municipalities are annotated. c-d, g-h, Cooling

patterns across 1-km² cells within these municipalities, showing the least equitable (c, g) and more equitable (d, h) configurations for SEP and permit type, respectively.

Discussion

Urban densification reduces land consumption but places greater pressure on the green spaces that provide ecosystem services[40]. Alongside the established population scaling of surface urban heat-island intensity[41], we find that vegetation cooling supply is systematically lower in more populous and denser areas, following a negative power-law relationship with population size and density, a pattern consistent with lower per-capita green space in more populous cities[42]. SCOPE simulates vegetation cooling for each 10-m pixel from its local vegetation characteristics, including canopy structure and leaf area, and residential exposure is calculated as the mean cooling across surrounding pixels. The negative scaling relationship therefore reflects the combined variation in the amount, spatial arrangement and biophysical properties of vegetation around residents' homes with population size and density. Shared infrastructure can serve larger populations without increasing in direct proportion to population size, creating economies of scale[43,44]. Vegetation cooling, by contrast, is spatially localized[45], making the proximity of vegetated surfaces to residents' homes consequential. Dense urban form therefore combines greater cooling demand with limited cooling supply.

Aggregate urban scaling can conceal who gains or loses across cities of different sizes. Previous work on socioeconomic scaling has shown that the upper tail of within-city distributions accounts for much of observed superlinear scaling, illustrating why population-wide exponents should be considered alongside within-city distributions[27]. Looking within cities is also important for urban cooling, as socially disadvantaged groups receive less green cooling across major European urban areas[46]. Our individual-level analysis shows that the scaling relationship itself is socially stratified. Low-SEP residents and residents at the lower end of local cooling distributions have a steeper negative scaling relationship with neighborhood density. The cooling penalty associated with density is therefore not shared evenly, making it a matter of distributive justice[7]. The individual records also show that cooling scaling varies among residence permit groups, extending the analysis beyond economic position to legal residence status. Residence status is particularly relevant here because permit type is closely linked to the prospect and duration of remaining in Switzerland[47], while the cooling benefit examined is tied to the residential environment.

Cooling inequality scales positively with population at both cell and municipality levels, across focal radii, and under both the Gini and Theil indices. Larger and denser urban areas therefore combine lower mean cooling with a more uneven distribution. The same positive population scaling has been reported for within-city green-space and thermal inequality across 11,210 urban centers worldwide[30], so the regularity is not confined to one country or to one way of measuring it. What individual-level records add is the social composition of that inequality. Our comparisons separate inequality within a social group from differences in mean cooling between groups. Lower-SEP residents receive less cooling, but their cooling is more homogeneous than that of higher-SEP residents. Temporary and permanent residents differ in mean cooling while showing similar within-group inequality. A low Gini can therefore indicate broadly shared low cooling rather than an equitable outcome, so inequality magnitude alone is insufficient to diagnose cooling equity. Building on a typology that paired income inequality with the social distribution of heat stress across 481 US cities[48], we combine Gini and CI to distinguish the magnitude of cooling inequality from its social direction. Residents aged 80 and above are particularly vulnerable to heat[49], yet separating them from those aged 65-79 shows that cooling is more often concentrated among the younger of the two groups (Extended Data Fig. 7). Within the older population, those at greatest risk are not those best served.

These findings should be interpreted in light of several limitations. Our cooling metric (GCoS) represents a simulated 24-hour mean of relative vegetation cooling supply rather than the air-temperature reduction experienced by residents. Accordingly, the model does not reproduce the full urban energy balance, including building shade, street-canyon geometry, and anthropogenic heat. The radiative, evapotranspirative and aerodynamic effects of vegetation can also vary by time of day and climate[50]. Soil moisture and stomatal conductance were held constant, so cooling may be overestimated where vegetation experiences water stress[51]. Beyond these modelling limitations, the scaling relationships were estimated over the relatively narrow population range of Swiss cities, limiting their extrapolation to large metropolitan systems. Exposure was also assigned to residential addresses and does not capture cooling at workplaces, schools or during travel; green-space exposure across these activity spaces may differ from that around the home[52]. Finally, we use "advantaged" and "disadvantaged" to denote relative residence security, socioeconomic position or heat vulnerability rather than to judge individual circumstances; adults aged 80 and above are placed in the latter group because of their greater physiological vulnerability.

Despite these limitations, our findings extend urban scaling research from aggregate quantities to the sociodemographic distribution of an environmental service. They also show why cooling interventions should not be allocated uniformly across municipalities. Tree-covered areas generally provide stronger cooling than treeless green spaces[53], although canopy expansion depends on tree survival, maturation, and maintenance[54]. Immediate protection through temporary shade structures, cooling centers and access to drinking water should accompany long-term canopy expansion[55]. Dense neighborhoods also require greening that uses buildings and paved public space. Green roofs and walls add vegetation without new open land, while street trees extending over paving and selective depaving make better use of existing public space[56]. The scaling analysis identifies how cooling supply and inequality change with population concentration, while the equity typology locates where these engineering and policy measures should be prioritized across municipalities and 1-km^2 neighborhoods.

Methods

Data

Meteorological data. Hourly meteorological variables were obtained from the ERA5 reanalysis dataset of the European Centre for Medium-Range Weather Forecasts (ECMWF), accessed via the Copernicus Climate Change Service (C3S)[57]. The dataset includes air temperature (2 m), relative humidity, surface pressure, 10 m wind speed, and downwelling shortwave and longwave radiation. These hourly fields provided boundary conditions for the vegetation cooling model. Background air temperature was characterized using predicted daily high-resolution air temperature data (100 m × 100 m) for Switzerland by Flückiger et al.[58] This dataset provides the thermal context for exposure assessment in Fig. 1 and is not an input to the cooling simulation.

Terrestrial surface data. Vegetation structure and land surface parameters were extracted from multiple satellite and national sources. The Leaf Area Index (LAI) (300 m resolution) was obtained from the Copernicus Global Land Service[59]. Canopy height data (1 m resolution, 2020) were provided by the Swiss National Forest Inventory and used to derive fractional canopy cover at 10-m resolution. Land cover and fractional vegetation surfaces were derived from the Swiss Habitat Map[60], which also provided delineations of inland water bodies (features < 0.1 km^2 excluded). Cultivated and agricultural surfaces were excluded from the fractional canopy cover calculation.

Demographic data. Person-level geo-coded demographic data (STATPOP; one record per resident, with residential coordinates at 1 m precision) were obtained from the Swiss Federal Statistical Office (STATPOP 2018), comprising age, gender, marital status, nationality, and residence permit type for all residents[61]. To ensure that every retained record refers to a genuine 1 m address point rather than a coordinate resolved only to the 100 m hectare grid, records were excluded where the coordinate fell on a 100 m grid node and at least 10 residents shared that node (53,480 residents at 773 nodes, 0.7% of records). Because individual-level income data are highly confidential in Switzerland, we used the area-based Swiss Neighborhood Index of Socioeconomic Position (Swiss-SEP) to represent relative socioeconomic position. The SEP was derived from the Swiss Neighborhood Index of Socioeconomic Position (Swiss-SEP 2015), an area-based deprivation indicator defined for

1.54 million micro-neighborhoods, each centered on a residential building and comprising the 50 nearest households by road-network distance. The index combines median rent, educational attainment, occupational class, and household crowding via principal component analysis, standardized to 0-100[62]. SEP was assigned to each individual via nearest-neighbor spatial join in EPSG:2056 coordinates and categorized into national quartiles. Municipalities classified as rural (“ländlich”) according to the Swiss Municipal Typology[63] were excluded to focus on urban and peri-urban areas. All data were accessed under a data-sharing agreement with the Swiss Federal Statistical Office and handled in compliance with Swiss data-protection regulations. To protect privacy and comply with the data-use agreement, individual records were used solely to derive residential exposure estimates. All reported results, including the equity typology, are aggregated to 1 km^2 cells or municipalities, precluding the identification of individuals or households.

Reference year. All analyses use 2018 as the reference year. STATPOP 2018 was the most recent release available when the study was designed, and 2018 was also a warm but not extreme Swiss summer, slightly exceeding the upper bound of the ±1 s.d. range around the 1990-2024 long-term mean (Supplementary Fig. 1). Using the same year for the demographic and meteorological inputs ensures that the population distribution and the modelled cooling supply refer to the same period. Canopy height (2020) and Swiss-SEP (2015) were the nearest available releases; both describe attributes that change slowly relative to the study period.

Modeling of urban green cooling supply

Cooling benefits were quantified using the Greening Cooling Services Index (GCoS), which integrates evapotranspirative (ECoS) and radiative (RCoS) components. In this study, we used the GCoS approach that was first established for Berlin[64] and then applied to many European cities[46]. The ET component was independently validated in a Swiss urban context (Basel) using eddy covariance tower measurements, achieving R^2 = 0.85-0.89 across two tower sites (obs = 1,652-1,697 half-hourly measurements per site, 2019/2021). GCoS is derived from the SCOPE (Soil Canopy Observation, Photosynthesis and Energy fluxes) model, a process-based approach that simulates canopy radiative transfer, heat fluxes, and energy balance[65]. Leaf area index and canopy height (see Terrestrial surface data) entered SCOPE as pixel-level inputs, driving the evapotranspirative and radiative components respectively;

fractional canopy cover, computed as the proportion of 1 m sub-pixels exceeding the 1 m height threshold within each 10 m cell, was applied in the second modelling stage to scale simulated fluxes to the vegetated proportion of each cell. GCoS represents the combined relative cooling potential of vegetation, expressed as a unitless index (0-1) standardized to a 24-hour mean for each 10 m pixel. As a bounded relative index, GCoS captures the spatial pattern of vegetation cooling supply rather than absolute air-temperature reduction. Because of Switzerland's substantial topographic variation, the hottest day in 2018 was identified independently for each canton based on daily mean air temperature, and the corresponding date's meteorological data were used as model input to calculate GCoS for that canton (Supplementary Table 4). Following the parameterization of ref.[46], stomatal conductance and soil moisture parameters were held constant in space and time at their default values, and irrigation was not represented. GCoS therefore represents potential cooling supply under non-water-limited conditions and may overestimate realized cooling where vegetation experiences soil-moisture stress. Because these parameters are spatially uniform, they shift the absolute level of GCoS but not its relative spatial distribution, on which all comparisons reported here are based.

Multi-radius extraction of cooling exposure

For each resident, GCoS was averaged within square moving windows centred on the residential address, with half-widths from 20 to 1,000 m in 20-m increments (50 radii), capturing cooling at both immediate residential and broader neighborhood scales. This half-width is termed the focal radius. Testing several window sizes rather than committing to one is recommended practice in greenspace exposure analysis[66], and a previous study found that canopy cooling varies with the radius at which canopy cover is measured, over radii of tens of meters[18]. The 20-m increments resolve near-home gradients while extending to the wider neighborhoods of compact Swiss cities. Cooling values were subsequently aggregated to 1 km^2 cells, municipalities, cantons, and biogeographic regions for multi-scalar analyses.

Classification of sociodemographic groups

Sociodemographic indicators were classified as follows: (1) Age: 0-25, 26-44, 45-64, 65-79, and 80+ years; (2) Residence permit: four groups reflecting legal residency status: Swiss citizens, permanent residents (C permit), long-term residents (B permit, residence permit for work and study more than 1 year), and short-term residents (L permit, normally short-term less than 1 year); (3) Gender: male and female; (4) Civil status: married, single, divorced, and widowed; (5) SEP: four groups derived by categorizing the continuous Swiss-SEP score (0-100) into national quartiles: Low (Q1), Lower-Middle (Q2), Upper-Middle (Q3), and High (Q4). Nationality was additionally classified as Swiss citizen, EU/EFTA national, or non-EU/EFTA national. We computed pairwise Spearman rank correlations among cell-level proportions of sociodemographic groups and mean socioeconomic position (Supplementary Fig. 2). Nationality was excluded from the main analysis owing to high correlation with residence permit type. Group definitions differ between the two analyses in the socioeconomic dimension by design. The scaling analysis (Fig. 3) contrasts the extremes of the SEP distribution, high (Q4) versus low (Q1), to characterize the steepest social gradient in cooling supply. For between-group comparisons of inequality (Fig. 4d-e), SEP was instead split at the median into upper (Q3-Q4) and lower (Q1-Q2) halves, so that the compared groups are mutually exclusive and jointly cover the full population, a condition for interpreting Gini and Theil as population-level distributional measures. Residence permit groups (settled: Swiss citizens and C-permit holders; temporary: B and L permit holders) are identical across both analyses.

Log-linear cooling gradient and saturation distance

Log-linear cooling gradient. To visualize how group-level cooling benefits vary with neighborhood extent, we fitted a log-linear model of the form $Coolingbenefit(r) = \alpha + \beta \cdot ln(r)$ to group-median cooling benefit at 50 focal radii (20-1,000 m in 20 m steps), where r is the focal radius in meters. The model was fitted by ordinary least squares. Fitted curves are shown in Fig. 2b.

Cooling saturation distance. The saturation distance (r_{95}) was derived from an exponential saturation model fitted independently to the group-median cooling profile. For each sociodemographic group, the model:

$$\text{Cooling benefit}(r) = a \cdot (1 - \exp(-b \cdot r)) \quad (1)$$

It was fitted by nonlinear least squares to the group-median cooling benefit at radii larger than 20 m (i.e., 40-1000 m in 20 m steps; up to 50,000 individuals per group), where a is the asymptotic maximum cooling and b is the rate parameter. The saturation distance was then derived analytically as:

$$r_{95} = \frac{-\ln(1-0.95)}{b} = \frac{\ln(20)}{b} \qquad (2)$$

Group differences in r_{95} were assessed by a permutation test, and bootstrap standard errors were estimated as described above. r_{95} values are shown in Extended Data Fig. 2a. Full model parameter estimates and standard errors per sociodemographic group are provided in Supplementary Table 5.

Multiple regression analysis

To disentangle independent sociodemographic associations with cooling, we estimated a pooled ordinary least squares (OLS) regression of individual-level vegetation cooling benefit at a focal radius of 100 m on all five sociodemographic indicators simultaneously. Categorical variables were dummy-coded with the following reference groups: age 65-79 years, Swiss citizens (permit type), high SEP, male (gender), and married (civil status). The model was estimated on n = 7,013,916 individuals with complete records across all indicators, after excluding missing, “Not specified”, and “Other” in residence permit categories. Cooling is assigned at the residential address, so individuals living at the same address are not independent observations. Standard errors were therefore clustered by residential address (1,148,138 clusters) using the CR1 finite-sample correction. Regression coefficients, 95% confidence intervals, and significance (t-test) were reported for each non-reference level. Model fit was assessed with R^2 and the F-statistic. Results are presented as a forest plot (Extended Data Fig. 3). The full regression table (β, SE, 95% CI, t, p, R^2, F-statistic) is provided in Supplementary Table 6.

Group comparisons and bootstrap significance testing

Group differences were assessed using outcome-specific resampling procedures. For cooling magnitude at a given focal radius (Fig. 2a), residential addresses were resampled with replacement (5,000 replicates), retaining all residents of each drawn address so that the estimand stays person-weighted while the address is the resampling unit. Pairwise group differences were recalculated in each replicate; 95% confidence intervals are the 2.5th and 97.5th percentiles of that distribution, and two-sided p-values are twice the smaller tail proportion around zero. For r_{95} (Extended Data Fig. 2a), individual cooling profiles from each group and its reference were pooled and randomly reassigned to their original sample sizes, capped at 50,000 individuals per group, with r_{95} refitted for each of 500 permutations; fewer permutations were used because every iteration requires refitting the nonlinear model. Bootstrap standard errors for r_{95} come from 200 within-group resamples. Both procedures use the add-one p-value (r + 1)/(B + 1), where r counts replicates at least as extreme as the observed difference and B the number of replicates, so the smallest attainable p-value is 1/501 for r95 and 1/5,001 for the address bootstrap. All comparisons used the reference groups defined above.

Density-stratified analysis

To examine whether sociodemographic disparities in cooling persist across different residential density contexts, rather than simply reflecting groups' differing distributions along the local density gradient, we stratified individuals into three density tertiles (Low, Medium and High) based on focal population at the 100-m residential scale. Focal population was computed for each 100-m grid cell as the sum of residents in the cell and its four cardinal neighbors (north, south, east and west). Cells with fewer than five residents were excluded. Tertile boundaries were defined globally across all urban and peri-urban individuals. Within each stratum, group medians and interquartile ranges of cooling at 100 m were computed, and pairwise bootstrap significance tests (n = 2,000 resamples; maximum 50,000 individuals per group) were performed against the same reference groups used in the national analysis. Results are presented in Extended Data Fig. 4. Median cooling and bootstrap p-values for each group-density stratum are provided in Supplementary Table 7.

Scaling law analysis of cooling

We modeled the scaling of vegetation cooling benefits with population size using log-log ordinary least squares (OLS) regression:

$$Y = \alpha N^{\beta} \tag{3}$$

where *Y* is the mean individual cooling benefit (or inequality metric) at a given focal radius, N is the population count, α is a normalization constant, and β is the scaling exponent. The scaling exponent β represents the elasticity of the outcome with respect to population; a negative β indicates that cooling (or inequality) declines with increasing urban density or city size. Analyses were conducted at two spatial levels. At the 1 km² cell level, N is the cell population count, equivalent to population density (persons km^{-2}). At the municipality level, N is the total municipal population. Spatial units with fewer than 20 persons were excluded.

Group-specific scaling models were estimated for three stratifications: (1) Distributional: Y was the 10^{th} percentile (P10) and 90^{th} percentile (P90) of individual cooling within each spatial unit; (2) SEP: Y was the mean cooling of residents in the top (high SEP) or bottom (low SEP) national quartile of Swiss-SEP scores; (3) Residence permit: Y was the mean cooling of settled residents (Swiss citizens and C permit holders) or temporary residents (B and L permit holders). Group-specific models were restricted to spatial units containing at least 3 persons in each group. To formally test whether scaling exponents differ between social groups, we applied a within-unit ratio regression:

$$\ln\left(\frac{Y_1}{Y_2}\right) \sim \ln(N) \quad (4)$$

where the slope $\Delta\beta = \beta_1 - \beta_2$.

All models were estimated with heteroskedasticity-consistent HC3 robust standard errors (R packages *sandwich* and *lmtest*). Scaling analyses at both spatial levels (1 km² and municipality) were repeated at 10 focal radii from 100 to 1,000 m in 100 m intervals to assess robustness across spatial extents.

Inequality and equity typology analysis

Inequality metrics. Cooling inequality within each spatial unit was quantified using two complementary metrics. The Gini index measures overall dispersion in individual cooling exposure and was computed using the sorted-ranks formula:

$$Gini = 1 + \frac{1}{n} - \left(\frac{2}{(n^2\mu)}\right)\sum_i (n + 1 - i)\, x_{(i)} \quad (5)$$

where $x_{(i)}$ is individual cooling exposures sorted in ascending order, μ is the mean cooling exposure, and *n* is the population size. The Theil index, an entropy-based alternative to the Gini, was computed as:

$$Theil = \frac{1}{n}\sum_i \left(\frac{x_i}{\mu}\right) ln\left(\frac{x_i}{\mu}\right) \quad (6)$$

where x_i is the cooling exposure of individual i and μ is the population mean. Both metrics were computed at the individual level within each spatial unit (1 km² cell and municipality) across all focal radii.

Concentration Index. The Concentration Index (CI) assesses whether cooling is systematically distributed in favor of socially advantaged or disadvantaged residents. We used the two-group rank-based formulation:

$$CI = \frac{\left(2(w_1 r_1 \mu_1 + w_2 r_2 \mu_2)\right)}{\mu} - 1 \quad (7)$$

where the population is divided into two groups, a socially advantaged group (group 1) and a socially disadvantaged group (group 2), defined separately for each indicator: upper 50% versus lower 50% SEP, permanent versus temporary residents, and the 65-79 versus 80+ age groups. Here w_1 and w_2 are the population shares of each group ($w_1 + w_2 = 1$), μ_1 and μ_2 are their mean cooling exposures, and μ is the overall mean cooling. The fractional ranks are assigned as $r_2 = w_2/2$ (disadvantaged group, ranked below) and $r_1 = w_2 + w_1/2$ (advantaged group, ranked above), placing the disadvantaged group at the lower end of the social rank distribution. A positive CI indicates that cooling is disproportionately concentrated among the advantaged group (pro-advantaged); a negative CI indicates higher cooling benefits among the disadvantaged group (pro-disadvantaged). A minimum of 5 individuals per group was required for CI computation.

Municipal-level equity diagnostics.

Each municipality was characterized by its Gini index (overall cooling dispersion) and CI (social bias in cooling). Municipalities were classified into four quadrants by whether their Gini exceeded the national mean and whether their CI was positive (pro-advantaged) or negative (pro-disadvantaged). High Gini combined with positive CI (upper-right quadrant) indicates that cooling is both unevenly distributed and concentrated among advantaged residents (least equitable); low Gini combined with negative CI (lower-left quadrant) reflects more equitable, pro-disadvantaged conditions. The same classification was applied at the 1 km² cell level to produce a neighborhood-level (1km²) national equity typology map.

Data availability

The vegetation and land-surface datasets used for modeling vegetation cooling benefit include the 1 m Vegetation Height Model from the National Forest Inventory (NFI, last accessed 30 October 2024; the old website is closed, and currently the dataset is available at https://www.envidat.ch/dataset/vegetation-height-model-nfi). The Leaf Area Index (LAI, 300 m) is from the Copernicus Global Land Service (https://land.copernicus.eu/en/products/vegetation/leaf-area-index-300m-v1.0). Habitat and land-cover data were derived from the Habitat Map of Switzerland (https://www.envidat.ch/#/metadata/habitat-map-of-switzerland). Meteorological variables used in the rSCOPE model were sourced from the ERA5 reanalysis produced by the Copernicus Climate Data Store (https://cds.climate.copernicus.eu/). Hourly variables included 2 m temperature, 10 m wind speed, surface pressure, total precipitation, downward shortwave and longwave radiation, and relative humidity. ERA5 data were accessed via the *ecmwfr* interface in R. The outcome datasets of cooling benefits from urban vegetation generated in this study are deposited in the ETH Zurich Research Collection (https://www.research-collection.ethz.ch/entities/researchdata/022ab0f4-18ef-4c3a-a7d3-3e206daaafbd, under embargo). The biogeographical regions of Switzerland were obtained from the Swiss Geographic Catalogue (https://www.geocat.ch/geonetwork/srv/eng/catalog.search#/metadata/fc110d43-cfbc-4029-a73c-f24bd67c9689). Geo-coded individual-level demographic data and socio-economic position data (Swiss-SEP) were obtained from Swiss Federal Statistical Office (https://www.bfs.admin.ch/bfs/en/home/statistiken/bevoelkerung/erhebungen/statpop.html). All demographic datasets above were accessed under a data-sharing agreement with the Swiss Federal Statistical Office, in compliance with the Swiss Federal Act on Data Protection (FADP) and applicable data confidentiality regulations. The record linkage was performed by the FSO, and the matched dataset was made available to the researchers in an anonymized/pseudonymized format and cannot be shared.

Code availability

Vegetation cooling was simulated with the SCOPE model as implemented in the rSCOPE R package (v1.0)[67]. All subsequent processing and analyses were performed in Python and R. Processing of the 1-m national canopy-height data, individual-level cooling extraction, and the bootstrap and permutation procedures was conducted on the ETH Zurich Euler high-performance computing cluster. The underlying individual-level records cannot be shared under the data agreement with the Swiss Federal Statistical Office. The analysis code, SCOPE modeling materials, and derived data will be made publicly available upon publication.

Acknowledgements

This work was supported by ETH Zurich. We gratefully acknowledge the Swiss Federal Statistical Office for its assistance in arranging the data agreement and transferring the STATPOP and Swiss National Cohort datasets. We also acknowledge the ETH High-Performance Computing Cluster (Euler) for providing the computational infrastructure. We acknowledge the support from the National Council for Scientific and Technological Development – CNPq under the programme Conhecimento Brasil Grant [446437/2024-7] to A.D.R.

Author Contributions

Y.C. and F.K. conceived and designed the study, with G.M., J.S., and J.G. contributing to conceptualization. Y.C. performed data collection and analysis, with contributions from A.D.R. to model development. Y.C. drafted the manuscript. J.G. acquired funding. F.K., G.M., J.S., A.D.R., M.J.S., D.A.M., R.B., and J.G. contributed to manuscript review and editing.

Competing interests

The authors declare no competing interests.

Declaration of Generative AI and AI-assisted technologies in the writing process

During the writing process of this work, we used OpenAI's ChatGPT to improve the language for clarity and conciseness. After using this tool, we thoroughly reviewed and edited the manuscript, and we take full responsibility for the content of the publication.

References

1. Richards, D. R. *et al.* Global variation in contributions to human well-being from urban vegetation ecosystem services. *One Earth* **5**, 522–533 (2022).
2. Wong, N. H., Tan, C. L., Kolokotsa, D. D. & Takebayashi, H. Greenery as a mitigation and adaptation strategy to urban heat. *Nat Rev Earth Environ* **2**, 166–181 (2021).
3. Anguelovski, I., Kotsila, P., Lees, L., Triguero-Mas, M. & Calderón-Argelich, A. From heat racism and heat gentrification to urban heat justice in the USA and Europe. *Nat Cities* **2**, 8–16 (2025).
4. Hsu, A., Sheriff, G., Chakraborty, T. & Manya, D. Disproportionate exposure to urban heat island intensity across major US cities. *Nat Commun* **12**, 2721 (2021).
5. Kleinschroth, F. *et al.* Global disparities in urban green space use during the COVID-19 pandemic from a systematic review. *Nat Cities* **1**, 136–149 (2024).
6. Li, Y. *et al.* Green spaces provide substantial but unequal urban cooling globally. *Nat Commun* **15**, 7108 (2024).
7. Wolch, J. R., Byrne, J. & Newell, J. P. Urban green space, public health, and environmental justice: The challenge of making cities 'just green enough'. *Landscape and Urban Planning* **125**, 234–244 (2014).
8. Tuholske, C. *et al.* Global urban population exposure to extreme heat. *Proceedings of the National Academy of Sciences* **118**, e2024792118 (2021).
9. Iungman, T. *et al.* Cooling cities through urban green infrastructure: a health impact assessment of European cities. *The Lancet* **401**, 577–589 (2023).
10. Zhao, J., Zhao, X., Wu, D., Meili, N. & Fatichi, S. Satellite-based evidence highlights a considerable increase of urban tree cooling benefits from 2000 to 2015. *Global Change Biology* **29**, 3085–3097 (2023).
11. Zhang, Y. *et al.* Transfer learning reveals large discrepancies between air and land surface temperatures in cities. *Nat Commun* **17**, 6890 (2026).
12. Wu, Z. & Chen, L. Optimizing the spatial arrangement of trees in residential neighborhoods for better cooling effects: Integrating modeling with in-situ measurements. *Landscape and Urban Planning* **167**, 463–472 (2017).
13. Yang, Y. *et al.* Regulation of humid heat by urban green space across a climate wetness gradient. *Nat Cities* **1**, 871–879 (2024).

14. Tsoka, S., Tsikaloudaki, A. & Theodosiou, T. Analyzing the ENVI-met microclimate model’s performance and assessing cool materials and urban vegetation applications–A review. *Sustainable Cities and Society* **43**, 55–76 (2018).
15. Huang, W. T. K. *et al.* Economic valuation of temperature-related mortality attributed to urban heat islands in European cities. *Nat Commun* **14**, 7438 (2023).
16. Sayyed, T. K. *et al.* Satellite data for environmental justice: a scoping review of the literature in the United States. *Environ. Res. Lett.* **19**, 033001 (2024).
17. Buzzelli, M. Modifiable Areal Unit Problem. in *International Encyclopedia of Human Geography (Second Edition)* (ed. Kobayashi, A.) 169–173 (Elsevier, Oxford, 2020). doi:10.1016/B978-0-08-102295-5.10406-8.
18. Ziter, C. D., Pedersen, E. J., Kucharik, C. J. & Turner, M. G. Scale-dependent interactions between tree canopy cover and impervious surfaces reduce daytime urban heat during summer. *Proceedings of the National Academy of Sciences* **116**, 7575–7580 (2019).
19. Wüstemann, H., Kalisch, D. & Kolbe, J. Access to urban green space and environmental inequalities in Germany. *Landscape and Urban Planning* **164**, 124–131 (2017).
20. Bettencourt, L. M. A. The Origins of Scaling in Cities. *Science* **340**, 1438–1441 (2013).
21. Bettencourt, L. & West, G. A unified theory of urban living. *Nature* **467**, 912–913 (2010).
22. Bettencourt, L. M. A., Lobo, J., Helbing, D., Kühnert, C. & West, G. B. Growth, innovation, scaling, and the pace of life in cities. *Proceedings of the National Academy of Sciences* **104**, 7301–7306 (2007).
23. Succar, R. & Porfiri, M. Urban scaling of firearm violence, ownership and accessibility in the United States. *Nat Cities* **1**, 216–224 (2024).
24. Xu, Y., Olmos, L. E., Abbar, S. & González, M. C. Deconstructing laws of accessibility and facility distribution in cities. *Science Advances* **6**, eabb4112 (2020).
25. Lu, M., Zhou, C., Wang, C., Jackson, R. B. & Kempes, C. P. Worldwide scaling of waste generation in urban systems. *Nat Cities* **1**, 126–135 (2024).
26. Lamsal, L. N., Martin, R. V., Parrish, D. D. & Krotkov, N. A. Scaling Relationship for NO2 Pollution and Urban Population Size: A Satellite Perspective. *Environ. Sci. Technol.* **47**, 7855–7861 (2013).
27. Arvidsson, M., Lovsjö, N. & Keuschnigg, M. Urban scaling laws arise from within-city inequalities. *Nat Hum Behav* **7**, 365–374 (2023).

28. Pandey, B., Brelsford, C. & Seto, K. C. Infrastructure inequality is a characteristic of urbanization. *Proceedings of the National Academy of Sciences* **119**, e2119890119 (2022).

29. Duran-Sala, M., Hendrick, M. & Manoli, G. Scaling intra-urban climate fluctuations. *Nat Cities* **3**, 545–554 (2026).

30. Huang, C. *et al.* A universal scaling law of intra-urban inequality. *Nat Commun* **17**, 6264 (2026).

31. Ballester, J. *et al.* Heat-related mortality in Europe during the summer of 2022. *Nat Med* **29**, 1857–1866 (2023).

32. Rousi, E., Kornhuber, K., Beobide-Arsuaga, G., Luo, F. & Coumou, D. Accelerated western European heatwave trends linked to more-persistent double jets over Eurasia. *Nat Commun* **13**, 3851 (2022).

33. Ceppi, P., Scherrer, S. C., Fischer, A. M. & Appenzeller, C. Revisiting Swiss temperature trends 1959–2008. *International Journal of Climatology* **32**, 203–213 (2012).

34. Federal Statistical Office. *Current Situation and Change: Key Population Figures, 2025 (Provisional Annual Figures)*. https://www.bfs.admin.ch/bfs/en/home/statistics/population/effectif-change.html (2026).

35. Chang, Y., Manoli, G., Ghazoul, J. & Kleinschroth, F. Socio-demographic disparities of heat exposure in affluent, aging, and diverse Swiss society. *Sustainable Cities and Society* **132**, 106813 (2025).

36. Lanza, K. *et al.* Heat vulnerability of Latino and Black residents in a low-income community and their recommended adaptation strategies: A qualitative study. *Urban Climate* **51**, 101656 (2023).

37. Randazzo, T., De Cian, E. & Mistry, M. N. Air conditioning and electricity expenditure: The role of climate in temperate countries. *Economic Modelling* **90**, 273–287 (2020).

38. Chi, D. *et al.* Residential tree canopy configuration and mortality in 6 million Swiss adults: a longitudinal study. *The Lancet Planetary Health* **9**, e186–e195 (2025).

39. Duarte Rocha, A., Vulova, S., van der Tol, C., Förster, M. & Kleinschmit, B. Modelling hourly evapotranspiration in urban environments with SCOPE using open remote sensing and meteorological data. *Hydrology and Earth System Sciences* **26**, 1111–1129 (2022).

40. Grêt-Regamey, A., Galleguillos-Torres, M., Dissegna, A. & Weibel, B. How urban densification influences ecosystem services—a comparison between a temperate and a tropical city. *Environ. Res. Lett.* **15**, 075001 (2020).
41. Manoli, G. *et al.* Magnitude of urban heat islands largely explained by climate and population. *Nature* **573**, 55–60 (2019).
42. Stuhlmacher, M., Frazier, A. E., Corya, I. & Yang, W. As cities grow larger, they may also become less green. *Journal of Land Use Science* **20**, 176–196 (2025).
43. Molinero, C. & Thurner, S. How the geometry of cities determines urban scaling laws. *J R Soc Interface* **18**, 20200705 (2021).
44. Shang, L. *et al.* Scaling of multiple functional facilities covering comprehensive processes in cities. *Cities* **145**, 104666 (2024).
45. Shah, A., Garg, A. & Mishra, V. Quantifying the local cooling effects of urban green spaces: Evidence from Bengaluru, India. *Landscape and Urban Planning* **209**, 104043 (2021).
46. Rocha, A. D. *et al.* Unprivileged groups are less served by green cooling services in major European urban areas. *Nat Cities* **1**, 424–435 (2024).
47. Wanner, P. Can Migrants' Emigration Intentions Predict Their Actual Behaviors? Evidence from a Swiss Survey. *Int. Migration & Integration* **22**, 1151–1179 (2021).
48. Chakraborty, T. C., Newman, A. J., Qian, Y., Hsu, A. & Sheriff, G. Residential segregation and outdoor urban moist heat stress disparities in the United States. *One Earth* **6**, 738–750 (2023).
49. Gallo, E. *et al.* Heat-related mortality in Europe during 2023 and the role of adaptation in protecting health. *Nat Med* **30**, 3101–3105 (2024).
50. Meili, N. *et al.* Tree effects on urban microclimate: Diurnal, seasonal, and climatic temperature differences explained by separating radiation, evapotranspiration, and roughness effects. *Urban Forestry & Urban Greening* **58**, 126970 (2021).
51. Gobatti, L., Bach, P. M., Maurer, M. & Leitão, J. P. Impact of soil moisture content on urban tree evaporative cooling and human thermal comfort. *npj Urban Sustain* **5**, 26 (2025).
52. Wei, L., Kwan, M.-P., Vermeulen, R. & Helbich, M. Measuring environmental exposures in people's activity space: The need to account for travel modes and exposure decay. *J Expo Sci Environ Epidemiol* **33**, 954–962 (2023).

53. Schwaab, J. *et al.* The role of urban trees in reducing land surface temperatures in European cities. *Nat Commun* **12**, 6763 (2021).
54. Esperon-Rodriguez, M. *et al.* Barriers and opportunities for resilient and sustainable urban forests. *Nat Cities* **2**, 290–298 (2025).
55. World Health Organization. Regional Office for Europe. *Heat-Health Action Plans: Guidance, Second Edition*. https://www.who.int/europe/publications/i/item/9789289062930 (2026).
56. McDonald, R. I. *et al.* Denser and greener cities: Green interventions to achieve both urban density and nature. *People and Nature* **5**, 84–102 (2023).
57. Hersbach, H. *et al.* The ERA5 global reanalysis. *Quarterly Journal of the Royal Meteorological Society* **146**, 1999–2049 (2020).
58. Flückiger, B. *et al.* Modelling daily air temperature at a fine spatial resolution dealing with challenging meteorological phenomena and topography in Switzerland. *Intl Journal of Climatology* **42**, 6413–6428 (2022).
59. Fuster, B. *et al.* Quality Assessment of PROBA-V LAI, fAPAR and fCOVER Collection 300 m Products of Copernicus Global Land Service. *Remote Sensing* **12**, 1017 (2020).
60. Price, B., Huber, N., Nussbaumer, A. & Ginzler, C. The Habitat Map of Switzerland: A Remote Sensing, Composite Approach for a High Spatial and Thematic Resolution Product. *Remote Sensing* **15**, 643 (2023).
61. Vienneau, D. *et al.* Transportation noise exposure and cardiovascular mortality: 15-years of follow-up in a nationwide prospective cohort in Switzerland. *Environment International* **158**, 106974 (2022).
62. Panczak, R., Berlin, C., Voorpostel, M., Zwahlen, M. & Egger, M. The Swiss neighbourhood index of socioeconomic position: update and re-validation. *Swiss Medical Weekly* **153**, 40028–40028 (2023).
63. Federal Statistical Office. Typology of municipalities and urban-rural typology. (2017).
64. Rocha, A. D., Vulova, S., Meier, F., Förster, M. & Kleinschmit, B. Mapping evapotranspirative and radiative cooling services in an urban environment. *Sustainable Cities and Society* **85**, 104051 (2022).
65. van der Tol, C., Verhoef, W., Timmermans, J., Verhoef, A. & Su, Z. An integrated model of soil-canopy spectral radiances, photosynthesis, fluorescence, temperature and energy balance. *Biogeosciences* **6**, 3109–3129 (2009).

66. Zare Sakhvidi, M. J. *et al.* Methodological guidance for selecting buffers in greenspace–health studies. *The Lancet Planetary Health* **9**, 101370 (2025).
67. Rocha, A. D. AlbyDR/rSCOPE: rSCOPE v1.0. https://doi.org/10.5281/zenodo.6204580 (2022) doi:10.5281/zenodo.6204580.

Extended Data

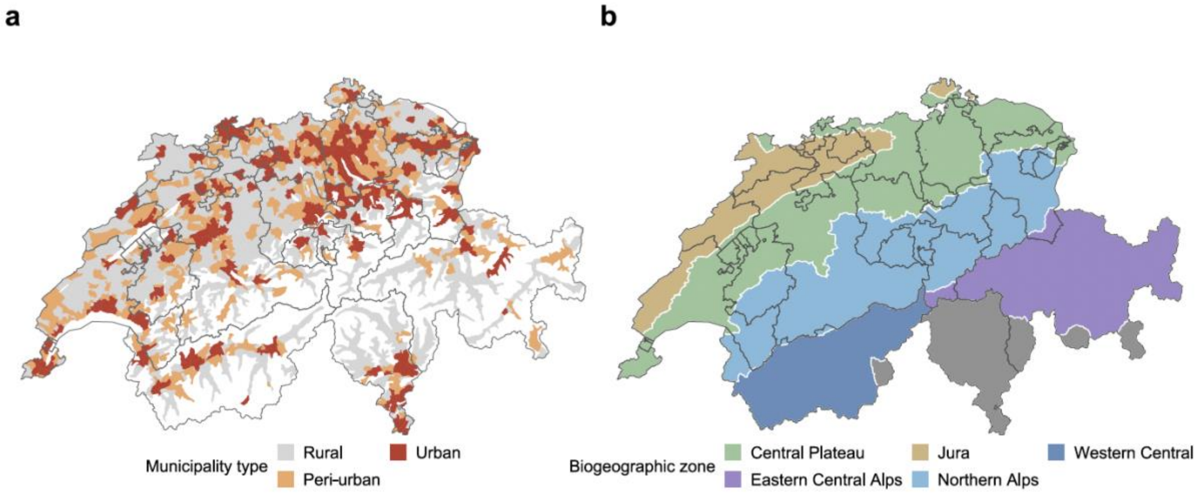

Extended Data Fig. 1. Study area overview. a, Classification of Swiss municipalities into Rural (grey), Peri-urban (orange), and Urban (red) categories based on the Swiss Federal Statistical Office urbanization typology. Cantonal borders are shown in dark grey. b, Biogeographic zones of Switzerland, comprising six regions: Central Plateau, Jura, Northern Alps, Western Central Alps, Eastern Central Alps, and Southern Alps.

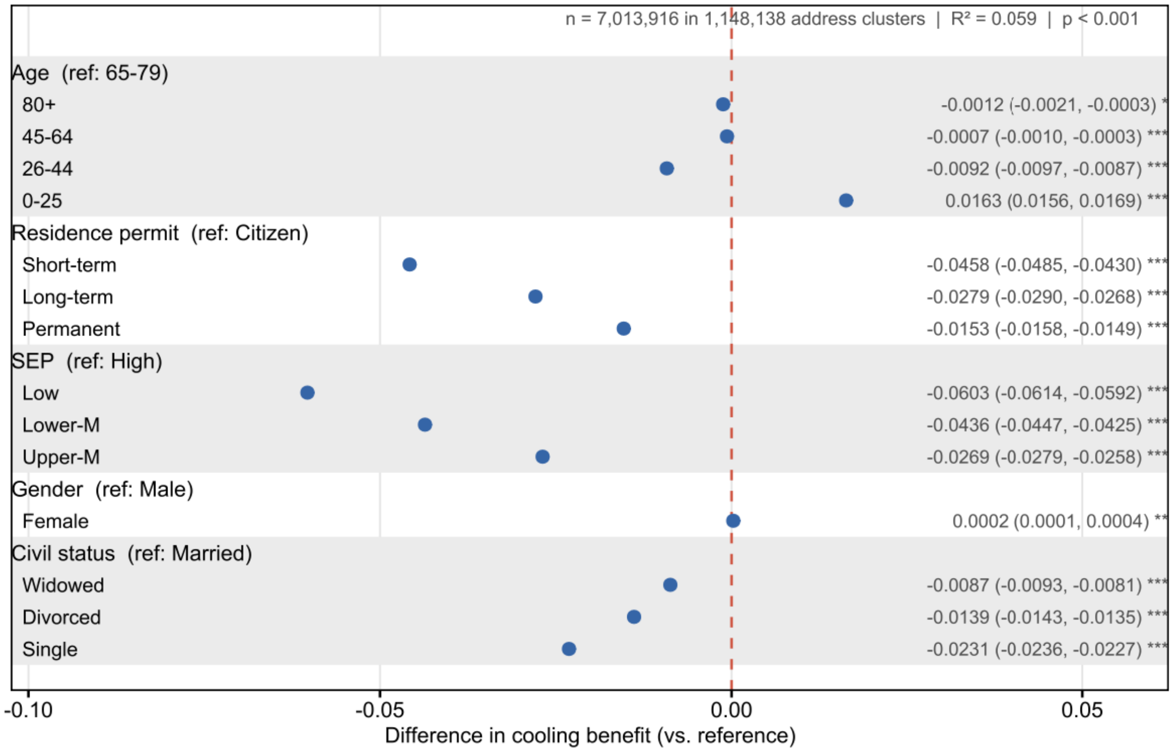

Extended Data Fig. 2. Multiple regression of individual-level cooling benefit (cooling benefits at 100 m focal radius) on five simultaneously included sociodemographic predictors. Forest plot of regression coefficients (β) for each non-reference group; 95% confidence intervals are given numerically beside each estimate. Reference groups are shown in parentheses. Significance: *** p < 0.001, ** p < 0.01, * p < 0.05, ns not significant.

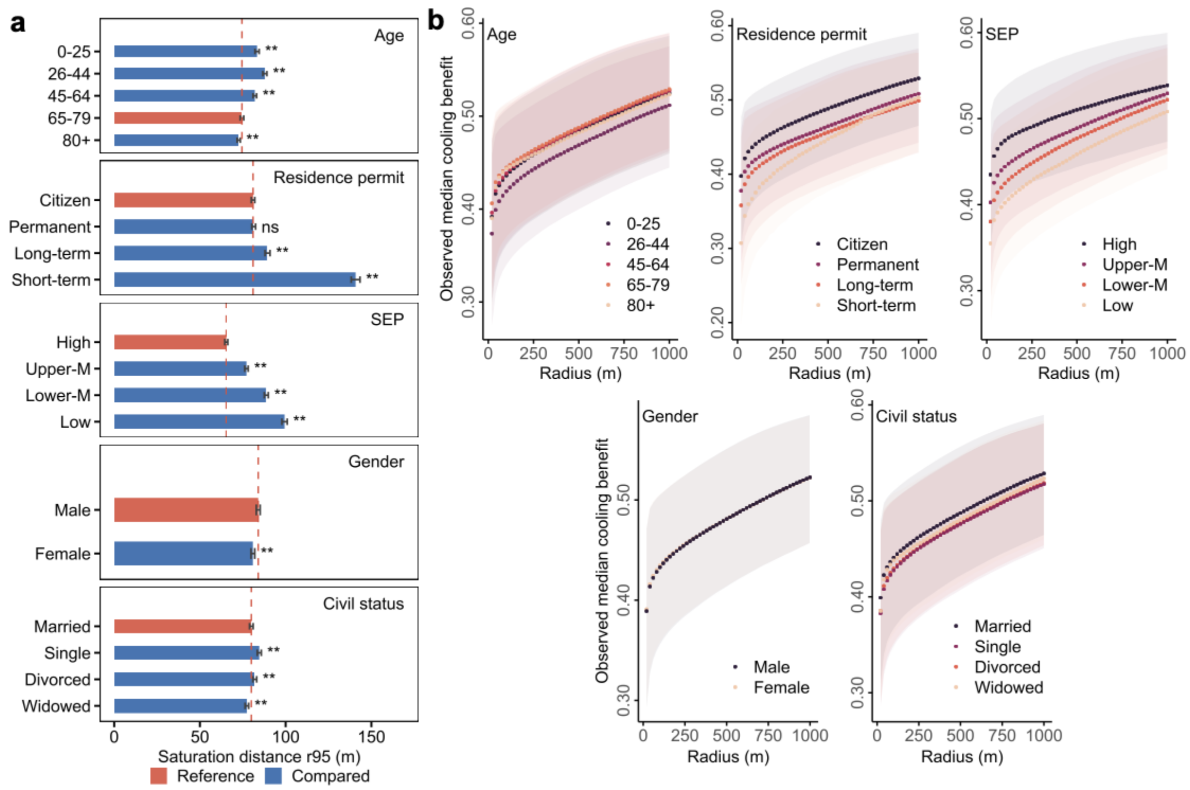

Extended Data Fig. 3. Saturation distance and observed cooling profiles across focal radii. a, Saturation distance (r_{95}), the focal radius at which 95% of the fitted asymptotic cooling benefit is reached, for each sociodemographic group. Bars show r_{95} and horizontal lines the interval $r_{95} \pm 1.96$ bootstrap standard errors (200 within-group resamples). Red marks the reference group for each indicator and blue the compared groups; the vertical dashed line marks the reference r_{95}. Significance stars refer to permutation tests against that reference (** $p < 0.01$, ns not significant); the permutation resolution is described in Supplementary Table 5, which also reports the full model parameters. b, Observed group-median cooling benefit at each focal radius from 20 to 1,000 m in 20 m steps, with shading from the 25th to the 75th percentile. These are the medians to which the log-linear curves in Fig. 2b are fitted.

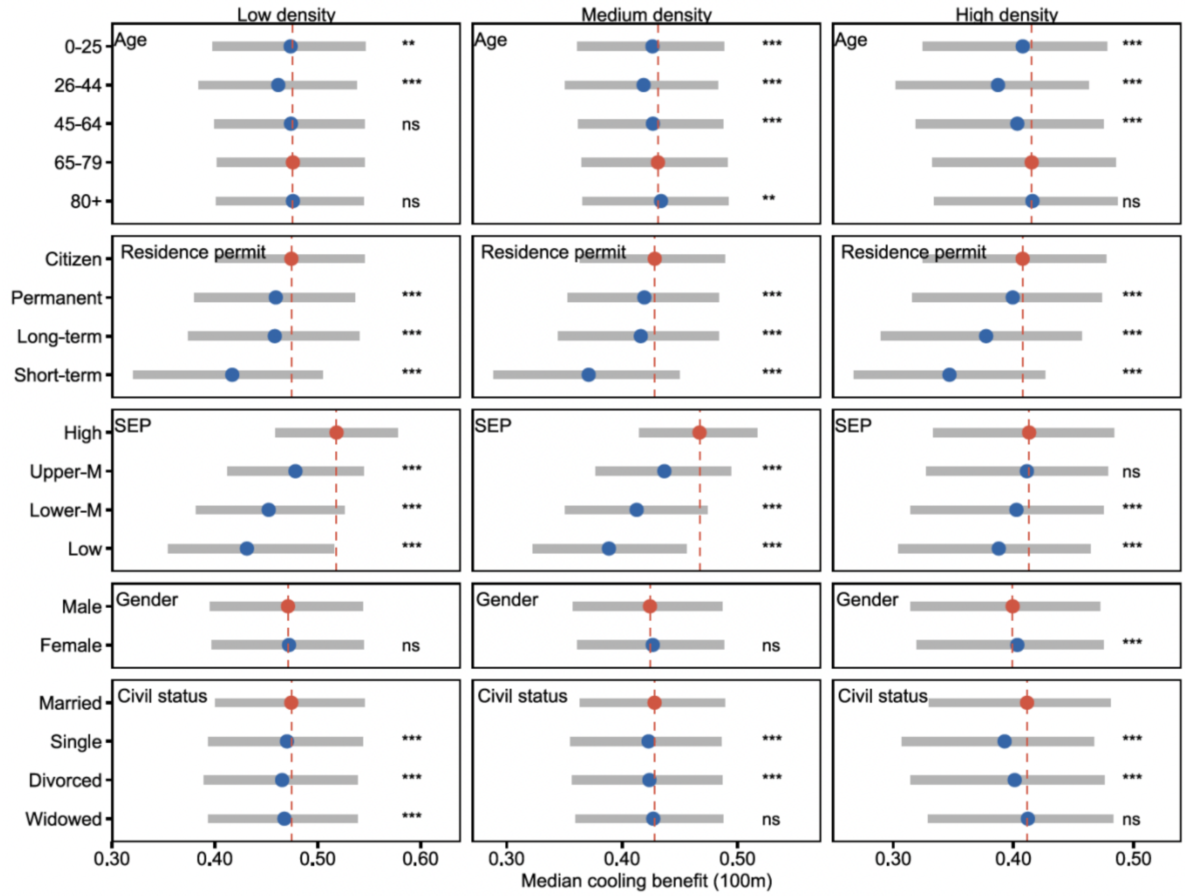

Extended Data Fig. 4. Density-stratified sociodemographic disparities in cooling benefit at a focal radius of 100 m. Groups are compared within three population density strata (Low, Medium, High) defined by tertiles of focal population at the 100 m scale. Points indicate group medians; horizontal bars denote interquartile ranges. Significance stars show bootstrap pairwise tests versus the reference group within each stratum (*** $p < 0.001$, ** $p < 0.01$, * $p < 0.05$, ns not significant).

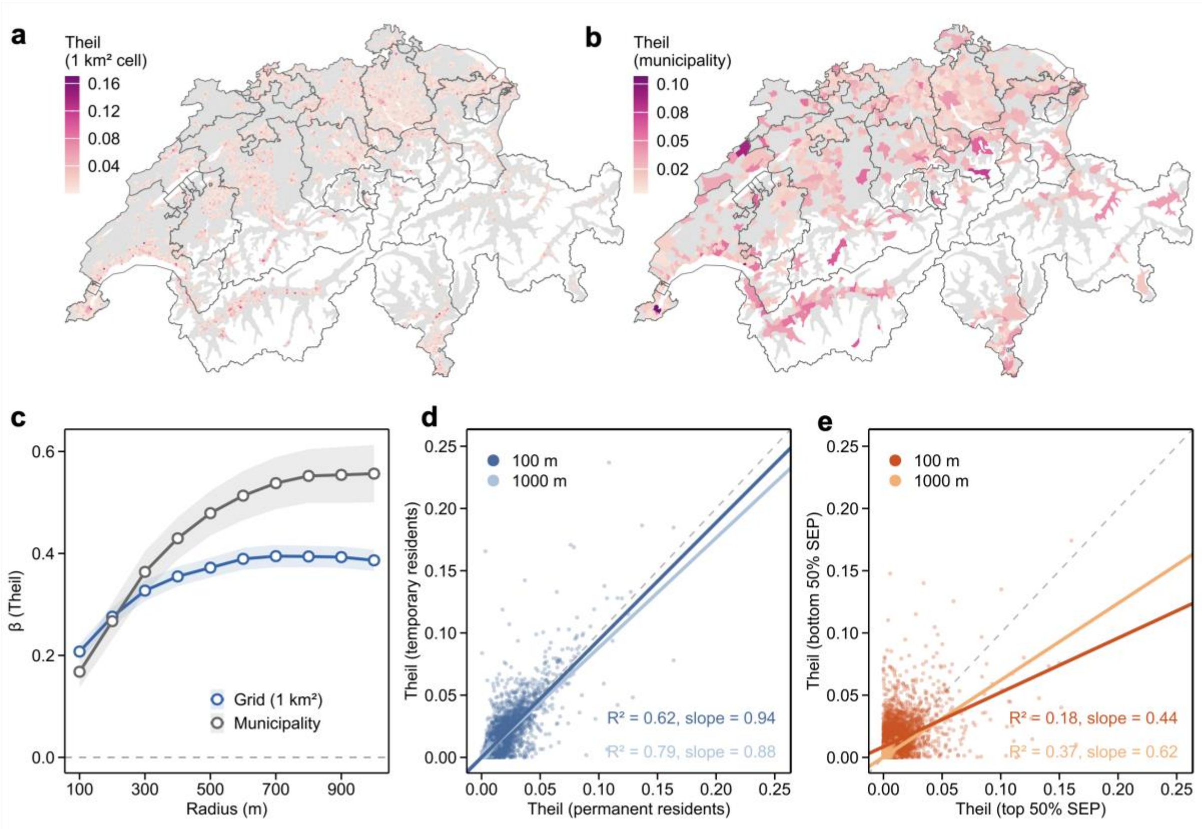

Extended Data Fig. 5. Urban scaling of cooling inequality measured by the Theil index. a-b, Spatial distribution of the Theil index at the $1km^2$ level (a) and municipality level (b), computed at a 100 m focal radius. c, Scaling exponent (β) of the Theil index against population size, estimated separately at the 1 km^2 cell (filled circles) and municipality (open circles) levels across focal radii from 100 to 1,000 m (100 m steps); the dashed horizontal line indicates $\beta = 0$; shaded ribbons show 95% confidence intervals. d-e, Pairwise comparison of subgroup Theil values at the 1 km^2 cell level, shown at focal radii of 100 m (dark) and 1,000 m (light), for permit type groups (d) and SEP groups (e); solid lines show ordinary least squares regression fits with reported slope and R^2 values.

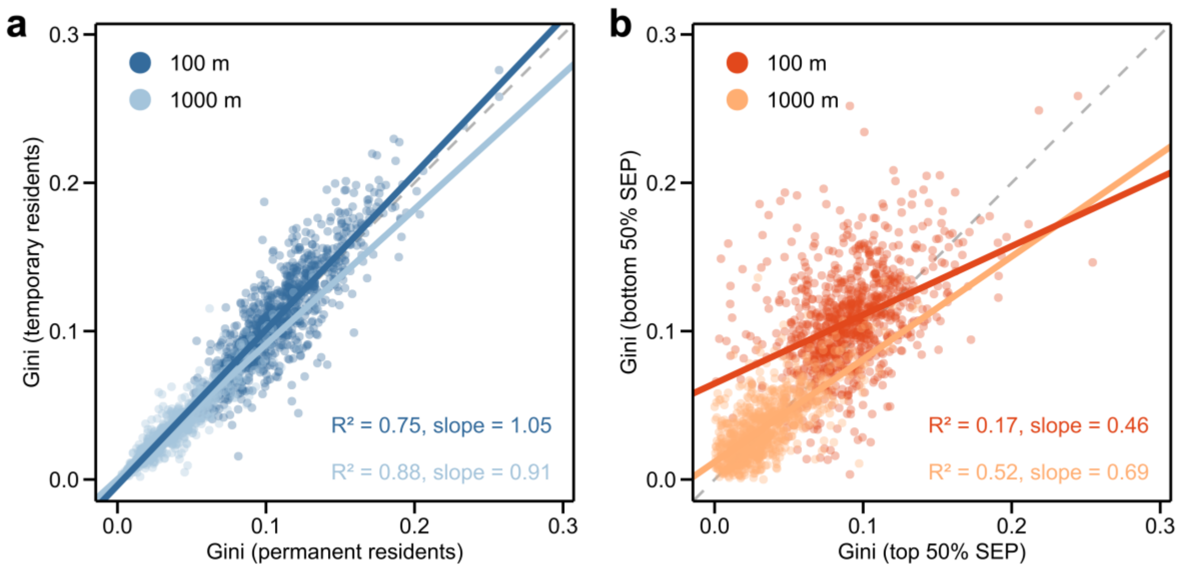

Extended Data Fig. 6. Pairwise comparison of cooling inequality (Gini index) between social groups at focal radii of 100 m and 1000 m at municipality level. a, Gini index for temporary residents versus permanent residents. b, Gini index for residents in the bottom 50% versus the top 50% of socioeconomic position (SEP). Dashed lines indicate the 1:1 equality line; solid lines show ordinary least squares regression fits with reported slope and R^2 values. Points above the 1:1 line indicate higher cooling inequality for the group on the y-axis.

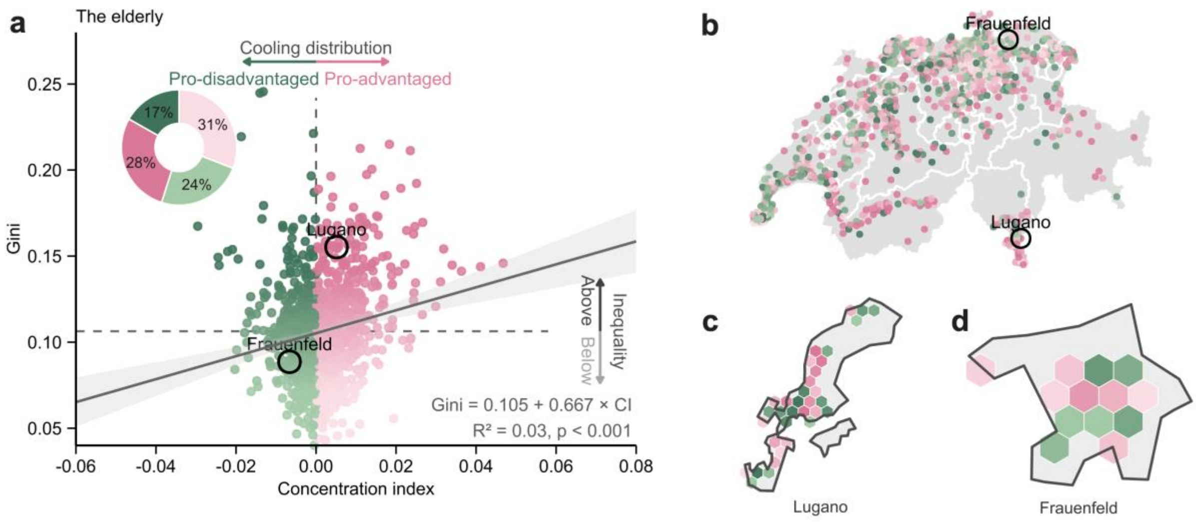

Extended Data Fig. 7. Municipal-level characterization of cooling inequality and equity for the elderly population (aged 65-79 versus 80+) across Swiss urban and peri-urban municipalities. a, each point represents one municipality in Gini-CI space. The Gini index is calculated from individual-level 100 m cooling within the combined population aged 65-79 and 80 and above, while the CI compares the two age groups using their population shares and mean individual cooling. Positive CI values indicate cooling concentrated among residents aged 65-79, whereas negative CI values indicate cooling concentrated among residents aged 80 and above. Dashed lines mark the mean Gini (horizontal) and CI = 0 (vertical); insets show the percentage of municipalities in each quadrant. The regression line shows the fitted linear relationship with 95% confidence interval. b, geographic distribution of municipalities colored by Gini-CI quadrant classification; pink = upper-right quadrant (above-average inequality, pro-advantaged); green = lower-left quadrant (below-average inequality, pro-disadvantaged). Canton boundaries are shown in white. c-d, Annotated examples illustrate contrasting municipal profiles: Lugano (Ticino) in the pro- advantaged, above-average inequality quadrant; Frauenfeld (Thurgau) in the pro-disadvantaged, below-average inequality quadrant.

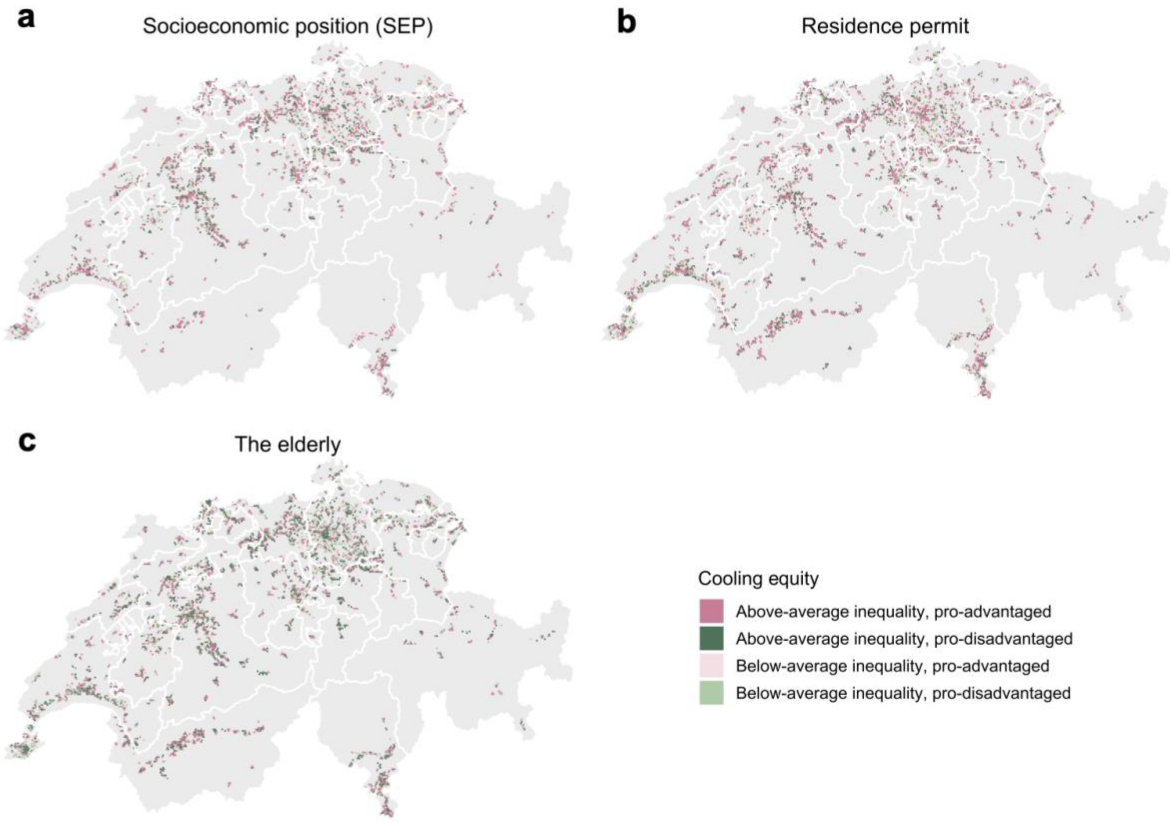

Extended Data Fig. 8. National distribution of cooling equity typology at the cell level (1 km²). Each cell is classified into one of four quadrants defined by its Gini index and Concentration Index. a, socioeconomic position (SEP). b, residence permit status. c, the elderly (residents aged 80+ versus 65-79). Canton boundaries shown in white.

Supplementary information

“Unequal scaling of urban vegetation cooling across sociodemographic groups”

Contents

Figures

Tables

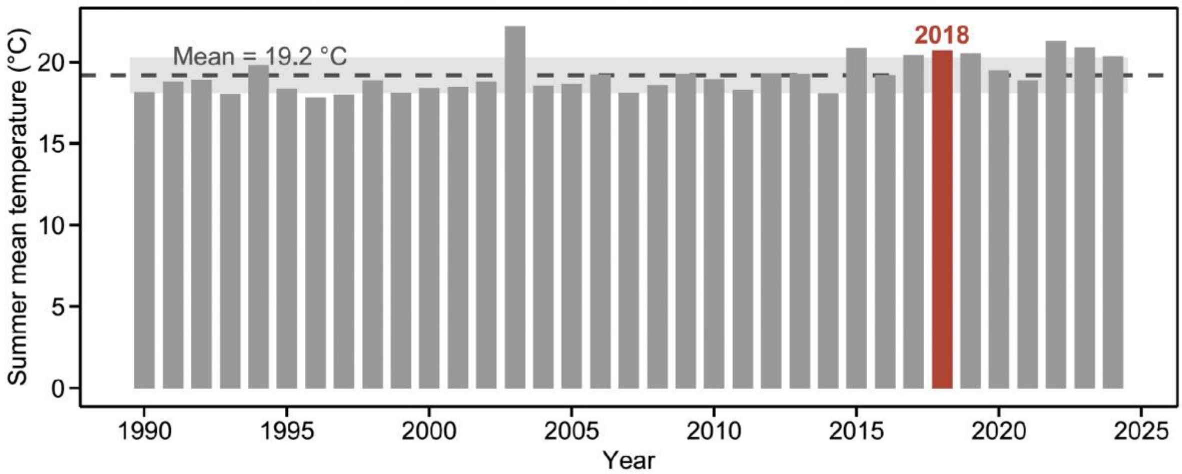

Supplementary Fig. 1. Historical summer (June-August) mean temperature across Switzerland from 1990 to 2024. Averaged across nine MeteoSwiss National Basic Climatological Network (NBCN) homogenized station records (Basel/Binningen, Bern/Zollikofen, Geneva/Cointrin, Lugano, Lucerne, Zürich/Fluntern, Sion, Neuchâtel, and St. Gallen). The dashed line indicates the 1990-2024 long-term mean (19.2 °C); the shaded band denotes ±1 standard deviation. The study year 2018 (red bar) slightly exceeds the upper bound of the ±1 standard deviation range, indicating a warm but not extreme summer relative to the recent climatological baseline.

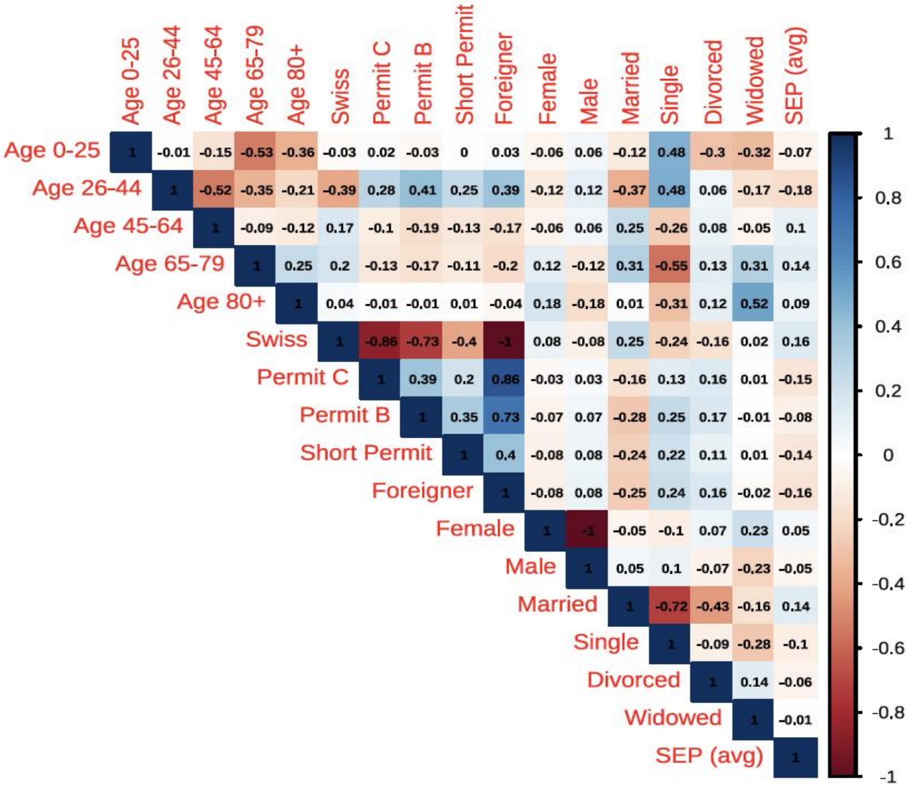

Supplementary Fig. 2. Pairwise Spearman rank correlation matrix among the five sociodemographic indicators used in the main analysis (age, gender, civil status, residence permit type, and socioeconomic position). Nationality and residence permit type show the highest inter-indicator correlation, motivating the exclusion of nationality from the main analysis.

Supplementary Table 1. Pairwise differences in median cooling benefit between sociodemographic groups at a focal radius of 100 m. For each indicator, every non-reference group is compared with the reference group (*italicized*). Differences are person-weighted medians computed over all residents. Confidence intervals were obtained by a cluster bootstrap that resamples residential addresses with replacement (5,000 replicates), carrying all residents of a sampled address, so that residents who share an address are not treated as independent observations. p-values are obtained by inverting the percentile interval. ΔGCoS = difference in median cooling benefit relative to the reference group; negative values indicate lower cooling than the reference.

Indicator	Group	Observed Δ GCoS	95% CI [lower, upper]	p-value
Age group	*65-79 (ref.)*	—	—	—
Age group	0-25	-0.0085	[-0.0091, -0.0078]	<0.001
Age group	26-44	-0.0253	[-0.0259, -0.0247]	<0.001
Age group	45-64	-0.0062	[-0.0067, -0.0058]	<0.001
Age group	≥80	-0.0011	[-0.0023, 0.0002]	0.102
Residence permit	*Swiss citizen (ref.)*	—	—	—
Residence permit	Long-term (B)	-0.0334	[-0.0347, -0.0320]	<0.001
Residence permit	Permanent (C)	-0.0207	[-0.0213, -0.0200]	<0.001
Residence permit	Short-term (L)	-0.0654	[-0.0704, -0.0607]	<0.001
Gender	*Male (ref.)*	—	—	—
Gender	Female	0.0018	[0.0015, 0.0019]	<0.001
Civil status	*Married (ref.)*	—	—	—
Civil status	Divorced	-0.0114	[-0.0119, -0.0108]	<0.001
Civil status	Single	-0.0132	[-0.0136, -0.0128]	<0.001
Civil status	Widowed	-0.0030	[-0.0041, -0.0019]	<0.001
Socioeconomic position	*High (ref.)*	—	—	—
Socioeconomic position	Low	-0.0723	[-0.0735, -0.0711]	<0.001
Socioeconomic position	Lower-middle	-0.0498	[-0.0510, -0.0487]	<0.001
Socioeconomic position	Upper-middle	-0.0304	[-0.0315, -0.0293]	<0.001

Supplementary Table 2. Urban scaling exponents (β) for cooling benefits at a 100 m focal radius, corresponding to Fig. 3. Models relate log cooling benefit to log population density at the 1 km² cell level and to log population size at the municipality level. β was estimated by OLS regression with HC3 robust standard errors. R^2 = coefficient of determination; p = two-sided p-value; n = number of spatial units.

Panel	Level	Group	β	R^2	p	n
a	1 km² cell	90th percentile	−0.044	0.135	<0.001	7434
a	1 km² cell	Whole population	−0.058	0.172	<0.001	7434
a	1 km² cell	10th percentile	−0.078	0.166	<0.001	7434
b	1 km² cell	Permanent residents	−0.047	0.105	<0.001	5806
b	1 km² cell	Temporary residents	−0.050	0.093	<0.001	5806
c	1 km² cell	High SEP	−0.041	0.062	<0.001	1997
c	1 km² cell	Low SEP	−0.067	0.119	<0.001	1997
d	Municipality	90th percentile	−0.013	0.013	<0.001	1021
d	Municipality	Whole population	−0.026	0.035	<0.001	1021
d	Municipality	10th percentile	−0.061	0.094	<0.001	1021
e	Municipality	Permanent residents	−0.022	0.027	<0.001	1017
e	Municipality	Temporary residents	−0.032	0.042	<0.001	1017
f	Municipality	High SEP	−0.011	0.006	0.052	689
f	Municipality	Low SEP	−0.023	0.018	0.001	689

Supplementary Table 3. Urban scaling exponents (β) for cooling inequality (Gini and Theil indices) at cell level (1 km²) and municipality level across focal radii (100-1000 m). β estimated by OLS regression of log(index) on log(population) with HC3 robust standard errors. 95% CI = heteroscedasticity-robust confidence interval; R^2 = coefficient of determination; p = two-sided p-value; n = number of spatial units.

Radius (m)	Level	Index	β	95% CI	R^2	p	n
100	Cell (1 km²)	Gini	0.126	[0.111, 0.140]	0.051	<0.001	8055
200	Cell (1 km²)	Gini	0.152	[0.141, 0.163]	0.125	<0.001	8053
300	Cell (1 km²)	Gini	0.177	[0.167, 0.188]	0.142	<0.001	8055
400	Cell (1 km²)	Gini	0.202	[0.187, 0.217]	0.118	<0.001	8058
500	Cell (1 km²)	Gini	0.210	[0.196, 0.224]	0.124	<0.001	8059
600	Cell (1 km²)	Gini	0.211	[0.199, 0.223]	0.165	<0.001	8057
700	Cell (1 km²)	Gini	0.217	[0.203, 0.231]	0.143	<0.001	8058
800	Cell (1 km²)	Gini	0.225	[0.209, 0.240]	0.115	<0.001	8060
900	Cell (1 km²)	Gini	0.219	[0.205, 0.233]	0.137	<0.001	8058
1000	Cell (1 km²)	Gini	0.215	[0.202, 0.229]	0.135	<0.001	8058
100	Municipality	Gini	0.081	[0.066, 0.097]	0.100	<0.001	1021
200	Municipality	Gini	0.138	[0.120, 0.156]	0.192	<0.001	1021
300	Municipality	Gini	0.191	[0.169, 0.212]	0.260	<0.001	1021
400	Municipality	Gini	0.228	[0.206, 0.250]	0.300	<0.001	1021
500	Municipality	Gini	0.255	[0.232, 0.278]	0.313	<0.001	1021
600	Municipality	Gini	0.274	[0.249, 0.299]	0.314	<0.001	1021
700	Municipality	Gini	0.287	[0.261, 0.313]	0.306	<0.001	1021
800	Municipality	Gini	0.293	[0.266, 0.320]	0.294	<0.001	1021
900	Municipality	Gini	0.293	[0.266, 0.321]	0.278	<0.001	1021
1000	Municipality	Gini	0.293	[0.264, 0.321]	0.267	<0.001	1021
100	Cell (1 km²)	Theil	0.208	[0.191, 0.224]	0.093	<0.001	8053
200	Cell (1 km²)	Theil	0.276	[0.258, 0.294]	0.119	<0.001	8055
300	Cell (1 km²)	Theil	0.327	[0.307, 0.347]	0.141	<0.001	8057
400	Cell (1 km²)	Theil	0.355	[0.336, 0.374]	0.154	<0.001	8057
500	Cell (1 km²)	Theil	0.372	[0.353, 0.392]	0.167	<0.001	8057
600	Cell (1 km²)	Theil	0.389	[0.368, 0.411]	0.154	<0.001	8060
700	Cell (1 km²)	Theil	0.395	[0.373, 0.417]	0.156	<0.001	8059
800	Cell (1 km²)	Theil	0.394	[0.373, 0.415]	0.159	<0.001	8057
900	Cell (1 km²)	Theil	0.393	[0.372, 0.414]	0.150	<0.001	8058
1000	Cell (1 km²)	Theil	0.387	[0.366, 0.407]	0.146	<0.001	8058

Radius (m)	Level	Index	β	95% CI	R^2	p	n
100	Municipality	Theil	0.168	[0.136, 0.200]	0.109	<0.001	1021
200	Municipality	Theil	0.267	[0.231, 0.303]	0.189	<0.001	1021
300	Municipality	Theil	0.364	[0.323, 0.405]	0.253	<0.001	1021
400	Municipality	Theil	0.430	[0.388, 0.471]	0.285	<0.001	1021
500	Municipality	Theil	0.479	[0.435, 0.523]	0.299	<0.001	1021
600	Municipality	Theil	0.513	[0.465, 0.562]	0.298	<0.001	1021
700	Municipality	Theil	0.538	[0.487, 0.589]	0.291	<0.001	1021
800	Municipality	Theil	0.552	[0.499, 0.605]	0.280	<0.001	1021
900	Municipality	Theil	0.554	[0.499, 0.609]	0.266	<0.001	1021
1000	Municipality	Theil	0.557	[0.500, 0.613]	0.256	<0.001	1021

Supplementary Table 4. Canton-specific peak heat dates used for SCOPE model simulations. For each of the 24 modelling regions covering all 26 Swiss cantons, the most extreme summer heat day in 2018 was identified as the date with the highest region-averaged mean air temperature (Ta mean, ERA5 reanalysis at 100 m resolution). Hourly SCOPE simulations were run for each region on its respective peak heat date to derive the Greening Cooling Services (GCoS) index. Appenzell Innerrhoden and Appenzell Ausserrhoden were treated as one modelling region; Basel-Stadt and Basel-Landschaft were likewise combined.

Canton	Peak Heat Date	Ta mean (°C)
Aargau	03 Aug 2018	25.8
Appenzell*	05 Aug 2018	23.3
Basel*	04 Aug 2018	27.1
Bern	04 Aug 2018	25.4
Fribourg	03 Aug 2018	25.2
Geneva	05 Aug 2018	25.7
Glarus	05 Aug 2018	20.1
Graubünden	05 Aug 2018	17.4
Jura	04 Aug 2018	25.9
Lucerne	03 Aug 2018	25.8
Neuchâtel	03 Aug 2018	24.5
Nidwalden	05 Aug 2018	18.1
Obwalden	05 Aug 2018	18.9
Schaffhausen	03 Aug 2018	25.8
Schwyz	05 Aug 2018	23.7
Solothurn	04 Aug 2018	26.2
St. Gallen	05 Aug 2018	24.3
Thurgau	31 Jul 2018	27.1
Ticino	31 Jul 2018	25.1
Uri	05 Aug 2018	17.2
Valais	05 Aug 2018	20.9
Vaud	05 Aug 2018	24.8
Zug	05 Aug 2018	23.7
Zurich	03 Aug 2018	26.9

Supplementary Table 5. Parameters of the exponential saturation model fitted to focal median cooling (GCoS) per sociodemographic group. a = asymptotic cooling plateau; b = rate constant (m^{-1}, reported $\times 10^{-3}$); r_{50} = half-saturation distance (m); r_{95} = distance at which 95% of asymptotic cooling is reached (m); SE(r_{95}) = bootstrap standard error (200 within-group resamples); Δr_{95} = r_{95}(group) − r_{95}(reference); p = permutation test (500 permutations). The permutation test uses 500 iterations, which resolves p-values no smaller than 0.002; p-values are therefore reported at a resolution of 0.01. Reference groups are *italicized*.

Indicator	**Group**	**a**	**b ($\times 10^{-3}$)**	**r_{50} (m)**	**r_{95} (m)**	**SE(r_{95})**	**Δr_{95} (m)**	**p-value**
Age group	*65-79 (ref.)*	*0.4900*	*40.2010*	*17.240*	*74.520*	*0.530*	—	—
Age group	0-25	0.4872	35.9520	19.280	83.330	0.620	8.810	<0.01
Age group	26-44	0.4727	34.0920	20.330	87.870	0.610	13.350	<0.01
Age group	45-64	0.4897	36.5240	18.980	82.020	0.540	7.500	<0.01
Age group	≥80	0.4857	41.2520	16.800	72.620	0.470	-1.900	<0.01
Residence permit	*Swiss citizen (ref.)*	*0.4915*	*36.9870*	*18.740*	*80.990*	*0.520*	—	—
Residence permit	Long-term (B)	0.4598	33.5030	20.690	89.420	0.750	8.420	<0.01
Residence permit	Permanent (C)	0.4685	36.8210	18.820	81.360	0.570	0.370	0.651
Residence permit	Short-term (L)	0.4554	21.2740	32.580	140.810	1.310	59.820	<0.01
Gender	*Male (ref.)*	*0.4835*	*35.6650*	*19.430*	*84.000*	*0.570*	—	—
Gender	Female	0.4835	37.0320	18.720	80.890	0.560	-3.100	<0.01
Civil status	*Married (ref.)*	*0.4906*	*37.4520*	*18.510*	*79.990*	*0.540*	—	—
Civil status	Divorced	0.4793	36.5320	18.970	82.000	0.570	2.010	<0.01
Civil status	Single	0.4795	35.4080	19.580	84.610	0.600	4.620	<0.01
Civil status	Widowed	0.4833	38.7180	17.900	77.370	0.530	-2.620	<0.01
Socioeconomic position	*High (ref.)*	*0.5117*	*45.8150*	*15.130*	*65.390*	*0.440*	—	—
Socioeconomic position	Low	0.4630	30.1480	22.990	99.370	0.800	33.980	<0.01
Socioeconomic position	Lower-middle	0.4812	33.7680	20.530	88.720	0.600	23.330	<0.01
Socioeconomic position	Upper-middle	0.4917	38.8260	17.850	77.160	0.510	11.770	<0.01

Supplementary Table 6. Multiple regression of individual-level cooling benefit (GCoS at 100 m focal radius) on five sociodemographic indicators simultaneously. Categorical variables are dummy-coded; reference groups are *italicized*. β = regression coefficient; SE = standard error, clustered by residential address; 95% CI = confidence interval; t = t-statistic; R^2 = coefficient of determination; F = F-statistic for overall model fit.

Indicator	Group	β	SE	95% CI [lower, upper]	t	p-value
Age group	*65-79 (ref.)*	*0.0000*	—	—	—	—
Age group	0-25	0.0163	0.0003	[0.0156, 0.0169]	48.65	<0.001
Age group	26-44	-0.0092	0.0003	[-0.0097, -0.0087]	-35.80	<0.001
Age group	45-64	-0.0007	0.0002	[-0.0010, -0.0003]	-3.35	<0.001
Age group	≥80	-0.0012	0.0005	[-0.0021, -0.0003]	-2.55	0.011
Residence permit	*Swiss citizen (ref.)*	*0.0000*	—	—	—	—
Residence permit	Permanent (C)	-0.0153	0.0002	[-0.0158, -0.0149]	-63.61	<0.001
Residence permit	Long-term (B)	-0.0279	0.0006	[-0.0290, -0.0268]	-48.79	<0.001
Residence permit	Short-term (L)	-0.0458	0.0014	[-0.0485, -0.0430]	-32.53	<0.001
Gender	*Male (ref.)*	*0.0000*	—	—	—	—
Gender	Female	0.0002	0.0001	[0.0001, 0.0004]	3.12	0.002
Civil status	*Married (ref.)*	*0.0000*	—	—	—	—
Civil status	Single	-0.0231	0.0002	[-0.0236, -0.0227]	-101.25	<0.001
Civil status	Divorced	-0.0139	0.0002	[-0.0143, -0.0135]	-64.87	<0.001
Civil status	Widowed	-0.0087	0.0003	[-0.0093, -0.0081]	-28.43	<0.001
Socioeconomic position	*High (ref.)*	*0.0000*	—	—	—	—
Socioeconomic position	Upper-middle	-0.0269	0.0005	[-0.0279, -0.0258]	-49.76	<0.001
Socioeconomic position	Lower-middle	-0.0436	0.0005	[-0.0447, -0.0425]	-80.48	<0.001
Socioeconomic position	Low	-0.0603	0.0005	[-0.0614, -0.0592]	-110.04	<0.001

Model: n = 7,013,916 individuals in 1,148,138 address clusters; intercept = 0.4828; R^2 = 0.0590; adj. R^2 = 0.0590; F(14, 7013901) = 31,412.4, p < 0.001

Supplementary Table 7. Density-stratified comparison of cooling benefit (GCoS) at a focal radius of 100 m. Individuals are stratified into low, medium, and high population density tertiles. For each stratum, non-reference groups are compared to the reference group by bootstrap resampling (2,000 resamples). GCoS = Green Cooling Services index; IQR = interquartile range [25th, 75th percentile].

Density stratum	Indicator	Group	n	Median GCoS	IQR [P25, P75]	p-value
Low	*Age group*	*65-79 (ref.)*	*329,610*	*0.476*	*[0.402, 0.546]*	—
Low	Age group	0-25	651,950	0.474	[0.398, 0.546]	0.001
Low	Age group	26-44	528,692	0.462	[0.385, 0.538]	<0.001
Low	Age group	45-64	702,432	0.474	[0.399, 0.546]	0.091
Low	Age group	≥80	117,735	0.476	[0.401, 0.545]	0.469
Low	*Residence permit*	*Swiss citizen (ref.)*	*1,899,552*	*0.474*	*[0.401, 0.546]*	—
Low	Residence permit	Long-term (B)	125,563	0.458	[0.375, 0.540]	<0.001
Low	Residence permit	Permanent (C)	269,371	0.459	[0.380, 0.536]	<0.001
Low	Residence permit	Short-term (L)	20,410	0.417	[0.321, 0.505]	<0.001
Low	*Gender*	*Male (ref.)*	*1,169,770*	*0.471*	*[0.395, 0.544]*	—
Low	Gender	Female	1,166,626	0.472	[0.397, 0.544]	0.234
Low	*Civil status*	*Married (ref.)*	*1,061,846*	*0.474*	*[0.400, 0.545]*	—
Low	Civil status	Divorced	174,437	0.465	[0.389, 0.539]	<0.001
Low	Civil status	Single	993,217	0.470	[0.394, 0.544]	<0.001
Low	Civil status	Widowed	106,797	0.468	[0.393, 0.539]	<0.001
Low	*Socioeconomic position*	*High (ref.)*	*540,291*	*0.518*	*[0.459, 0.578]*	—
Low	Socioeconomic position	Low	641,016	0.431	[0.355, 0.515]	<0.001
Low	Socioeconomic position	Lower-middle	601,156	0.452	[0.382, 0.526]	<0.001
Low	Socioeconomic position	Upper-middle	553,933	0.478	[0.412, 0.544]	<0.001
Medium	*Age group*	*65-79 (ref.)*	*308,666*	*0.431*	*[0.365, 0.491]*	—
Medium	Age group	0-25	627,661	0.426	[0.361, 0.488]	<0.001
Medium	Age group	26-44	627,412	0.419	[0.351, 0.483]	<0.001
Medium	Age group	45-64	636,732	0.427	[0.362, 0.487]	<0.001
Medium	Age group	≥80	129,492	0.434	[0.366, 0.492]	0.008
Medium	*Residence permit*	*Swiss citizen (ref.)*	*1,702,026*	*0.428*	*[0.364, 0.489]*	—
Medium	Residence permit	Long-term (B)	191,870	0.416	[0.344, 0.484]	<0.001
Medium	Residence permit	Permanent (C)	399,661	0.419	[0.353, 0.484]	<0.001
Medium	Residence permit	Short-term (L)	18,109	0.371	[0.289, 0.450]	<0.001
Medium	*Gender*	*Male (ref.)*	*1,149,196*	*0.424*	*[0.358, 0.487]*	—
Medium	Gender	Female	1,186,828	0.427	[0.361, 0.488]	0.102

Density stratum	**Indicator**	**Group**	**n**	**Median GCoS**	**IQR [P25, P75]**	**p-value**
Medium	*Civil status*	*Married (ref.)*	*975,432*	*0.428*	*[0.364, 0.489]*	—
Medium	Civil status	Divorced	206,064	0.424	[0.356, 0.487]	<0.001
Medium	Civil status	Single	1,037,931	0.423	[0.356, 0.486]	<0.001
Medium	Civil status	Widowed	116,484	0.427	[0.359, 0.488]	0.650
Medium	*Socioeconomic position*	*High (ref.)*	*511,177*	*0.467*	*[0.415, 0.517]*	—
Medium	Socioeconomic position	Low	694,703	0.389	[0.323, 0.456]	<0.001
Medium	Socioeconomic position	Lower-middle	569,738	0.413	[0.351, 0.474]	<0.001
Medium	Socioeconomic position	Upper-middle	560,406	0.437	[0.377, 0.494]	<0.001
High	*Age group*	*65-79 (ref.)*	*254,228*	*0.415*	*[0.332, 0.485]*	—
High	Age group	0-25	629,198	0.408	[0.325, 0.478]	<0.001
High	Age group	26-44	755,330	0.387	[0.302, 0.462]	<0.001
High	Age group	45-64	565,495	0.403	[0.319, 0.475]	<0.001
High	Age group	≥80	111,888	0.416	[0.334, 0.487]	0.916
High	*Residence permit*	*Swiss citizen (ref.)*	*1,450,300*	*0.408*	*[0.325, 0.477]*	—
High	Residence permit	Long-term (B)	293,098	0.377	[0.290, 0.457]	<0.001
High	Residence permit	Permanent (C)	512,468	0.399	[0.316, 0.473]	<0.001
High	Residence permit	Short-term (L)	22,401	0.347	[0.267, 0.426]	<0.001
High	*Gender*	*Male (ref.)*	*1,137,554*	*0.399*	*[0.314, 0.472]*	—
High	Gender	Female	1,184,656	0.403	[0.319, 0.475]	<0.001
High	*Civil status*	*Married (ref.)*	*847,927*	*0.411*	*[0.330, 0.481]*	—
High	Civil status	Divorced	215,703	0.401	[0.314, 0.476]	<0.001
High	Civil status	Single	1,159,855	0.393	[0.307, 0.467]	<0.001
High	Civil status	Widowed	98,624	0.412	[0.329, 0.483]	0.553
High	*Socioeconomic position*	*High (ref.)*	*402,319*	*0.413*	*[0.333, 0.484]*	—
High	Socioeconomic position	Low	839,128	0.388	[0.304, 0.464]	<0.001
High	Socioeconomic position	Lower-middle	569,227	0.403	[0.315, 0.475]	<0.001
High	Socioeconomic position	Upper-middle	511,536	0.411	[0.328, 0.479]	0.228